SLAC – PUB – 4356
June 1987
T/AS

Is the Universe Closed by Baryons? Nucleosynthesis with a Late Decaying Massive Particle*

SAVAS DIMOPOULOS

Department of Physics

Stanford University, Stanford, California, 94305

RAHIM ESMAILZADEH

Stanford Linear Accelerator Center

Stanford University, Stanford, California, 94305

LAWRENCE J. HALL

Department of Physics

University of California, Berkeley, California, 94720

GLENN D. STARKMAN

Department of Physics

Stanford University, Stanford, California, 94305

Submitted to *The Astrophysical Journal*

* Work supprted in part by the Department of Energy, contract DE-AC03-76F00515.

ABSTRACT

A late decaying ($\tau > 10^5 sec$), massive ($M \gtrsim 10$ GeV) particle initiates a new phase of nucleosynthesis in the keV era. Light element production takes place when the hadronic decay products interact with the ambient protons and ^4He causing hadronic showers and ^4He hadrodestruction. The primordial abundances of D, ^3He, ^6Li and ^7Li are given by the fixed points of the corresponding rate equations in which hadroproduction balances photodestruction. Since fixed points erase all previous memory, the primordial abundances of these elements are completely independent of the physics before the keV era, whose only important role is to provide at least the observed abundance of ^4He. Any overabundance of ^4He is subsequently hadrodissociated. The primordial element abundances are in agreement with observations; furthermore they are independent of $\Omega_B h_o^2$ for a very broad range of $\Omega_B h_o^2$ which includes the previously forbidden range $0.03 \leq \Omega_B h_o^2 \leq 1.1$. An ideal candidate for the late decaying particle may be the gravitino.

1. Introduction

One of the most fascinating consequences of recent observational cosmology is that at least 90% of the matter in the universe is invisible. This invisible or "dark matter" could consist of the usual baryons and leptons in states that do not radiate or absorb with sufficient intensity to be observable at present. Alternatively, it could consist of new particles that do not emit electromagnetic radiation. The most compelling reason in favor of the latter non-baryonic alternative comes from primordial nucleosynthesis (Peebles 1966; Wagoner 1967; Wagoner 1968; Wagoner et al 1967; Yang et al 1984; Primack 1984); its successful implementation requires that $0.014 < \Omega_B h_o^2 < 0.03$. If $\Omega_B h_o^2$ is larger than 0.03 then ^4He and ^7Li are overproduced and D is underproduced (eg. Wagoner 1967).

Other arguments against baryonic dark matter arising from distortions of the microwave background radiation (where adiabatic perturbations are assumed) and the separation of visible from invisible matter are less solid (Primack 1984). In fact, recent observations of the large scale structure of the universe have led Peebles (Peebles 1987a,b) to consider purely baryonic universes; similarly Blumenthal, Faber, Flores and Primack (Blumenthal et al 1986) and Blumenthal, Dekel and Primack (Blumenthal et al 1987) have considered theories with $\Omega_B h_o^2 > 0.03$.

We are aware of two classes of attempts to reconcile nucleosynthesis with $\Omega_B = 1$ using particle physics. Applegate, Hogan and Scherrer (Applegate et al 1987) and Alcock, Fuller and Mathews (Alcock et al 1987) have shown that baryon segregation and neutron diffusion after the QCD phase transition lead to distinct regions of nucleosynthesis. With suitable choice of unknown QCD

parameters the net yields of the light elements in an $\Omega_B = 1$ universe could be made to agree with observation, except that ^7Li was overproduced by two or three orders of magnitude. The importance of this work is that it introduces no new physics to the standard model. If the unknown QCD parameters are indeed in the range chosen by these authors, this could be the way standard nucleosynthesis operates. In practice it is very difficult to make thoroughly convincing calculations using these ideas.

A second class of attempts to reconcile $\Omega_B = 1$ with nucleosynthesis is that of Audouze et al (Audouze et al 1983) and Dominguez-Tenreiro (Dominguez-Tenreiro 1987). Audouze et al try to solve the deuterium underproduction problem by introducing a late radiatively decaying particle whose decay products lead to photodissociation of ^4He into D. Unfortunately, they cannot simultaneously account for the ^4He, D and ^3He abundances. In particular, we will show that such scenarios with purely radiatively decaying X's neccessarily lead to either too much ^3He or too much ^4He.

Dominguez-Tenreiro claims to have a positive scenario using only photodissociation and anti-nucleons; however, he ignores several dominant processes, including:

a)photodissociation of the overabundant mass seven elements, the only process that can sufficiently reduce their abundance without getting rid of ^4He ;

b) hadronic showers, the main source of D, ^3H, ^3He, ^6Li, ^7Li, and ^7Be.

Our general framework is much broader than the case $\Omega_B = 1$, or even the standard big bang. It applies to any theory which, in the 10 keV era ($t \simeq 10^4 sec$), has an overabundance of ^4He and is independent of the pre 10 keV abundances of the remaining elements . In such a theory, we add a long lived ($\tau \gtrsim 10^5 sec$)

massive ($M \gtrsim 10\text{GeV}$) particle X that decays in the few keV era and whose general properties are stated in the next section. The baryonic decay products of X interact with the ambient protons and alpha particles and cause nuclear chain reactions that lead to the production of the light nuclei D, ^3He, ^6Li, ^7Li and reduction of the previously overabundant ^4He. These light nuclei are in turn photodissociated by the radiation triggered by the X decay. The rate equations describing hadron and photon induced production and destruction of the light elements D, ^3He, ^6Li, ^7Li reach their fixed points for a very wide range of parameters. Since fixed point behavior erases all memory of initial conditions, the abundances of D, ^3He, ^6Li, ^7Li are completely independent of the physics that went on before the decay of the X particle. The fixed points are essentially determined by nuclear physics and do not depend on the properties of the X for a wide range of its parameters. Furthermore, the ratios of these abundances turns out to be independent of $\Omega_B h_o^2$ for a very large range of $\Omega_B h_o^2$ that includes the previously forbidden range $0.03 < \Omega_B h_o^2 \leq 1.1$. Thus, the agreement of these *ratios* with the relevant observations is a nontrivial test of these ideas. The absolute magnitude of the primordial abundances of D, ^3He, ^6Li and ^7Li does depend on one combination of the properties of X. Another combination is fixed by the requisite amount of hadrodestruction of the initially overabundant ^4He.[1]

---

1 The necessary amount of ^4He hadrodestruction depends on $\Omega_B h_o^2$. If $\Omega_B h_o^2 = 1$ then we need to hadrodissociate approximately 15% of the ^4He. If $\Omega_B h_o^2 < 1$ we need to hadrodestroy less. Our fractional abundances of ^3He, ^6Li and ^7Li are given by the fixed point condition and do not depend on $\Omega_B h_o^2$.

These two combinations completely determine the primordial abundances of D, ^3He, ^4He, ^6Li and ^7Li in our framework.

In section 2 we introduce the general requisite properties of the X particle. In section 3 we describe the observations against which we must compare our predictions. In section 4 we set up the formalism for the study of the hadronic showers, electromagnetic showers, and the nuclear processes that are triggered by the decay products of X in the hot ambient plasma. In section 5 we present the analytic solutions of the rate equations that demonstrate the aforementioned fixed point behavior, $\Omega_B h_o^2$ independence etc. In section 6 we present the results of numerical simulations which confirm and refine our analytic fixed point estimates. In section 7, we contrast our predictions with those of Standard Big Bang Nucleosynthesis, and identify ways in which their differences may be tested. Finally, in section 8 we summarize our results and present our conclusions.

2. Properties of the Decaying Particles

In this section we describe the properties of the particle X whose decays are responsible for altering the light element abundances. The element synthesis depends on the lifetime τ_X, the baryonic branching ratio in X decay r_B, the mass M_X, and the abundance relative to photons f_X° which X's have before they decay. We will discuss each of these parameters later. While the spin of X is unimportant, assumptions must be made about the other quantum numbers. For simplicity we will assume that it is a color singlet and electrically neutral.

As stressed in the introduction, our framework is independent of physics before 10keV, so long as ^4He is overproduced. However, for simplicity, we take the X particle lifetime to be $> 10^4$ seconds in order to ensure that X decays are late enough not to substantially disturb the conventional era of nucleosynthesis. In order not to distort the cosmic background radiation, we take $\tau_X < 10^9$ seconds (Silk and Stebbins, 1983). In fact our results show that τ_X lies in the range of $2 - 9 \times 10^5$ sec.

In the analysis of this paper we assume that X does not carry baryon number and does not have a large scattering cross-section with protons and neutrons. This assumption is necessary if $f_X^\circ \gtrsim f_B = n_B/n_\gamma$,[2] but is unnecessary for

---

2 If X carries baryon number and $f_X \gtrsim f_B$, then its decays will dilute ^4He by more than a factor of two. If X has a large scattering cross section with nucleons, then our hadronic shower calculations are altered.

$f_X^o \ll f_B$.[3]

Our results show that r_B should be in the approximate range of $\mathcal{O}(10^{-5})$ to $\mathcal{O}(1)$. It is reasonable to be anywhere in this range. X could decay directly to a final state containing baryons, in which case $r_B = \mathcal{O}(1)$, or such a decay might involve loops or virtual intermediate states, $r_B = \mathcal{O}(10^{-5} - 10^{-3})$.

The X mass must be larger than twice the proton mass so that it can decay baryonically. Our results also show that there is an upper bound to M_X of order 10^6 GeV; hence, the X particle is very long lived for its mass. It is most reasonable that X not have renormalizable interactions with quarks and leptons at the weak scale. Rather this long lifetime can arise naturally from a dimension 6 operator at the intermediate scale, or a dimension 5 operator at the Planck scale or Grand Unified scale. A familiar particle with its mass and lifetime in this range is the gravitino. Successful gravitino cosmologies with $0.1 \leq \Omega_B h_o^2 \leq 1$ are discussed elsewhere (Dimopoulos et al 1987).

Our results show that f_X^o/f_B should be in the range $\mathcal{O}(10^{-3})$ to $\mathcal{O}(10^2)$. Such an abundance may have an origin related to the cosmic baryon asymmetry, in which case $f_X^o \sim f_B$ is reasonable. Alternatively if $M_X < M_W$, then a weak annihilation rate would give acceptable values for f_X^o. Another possibility is that X has only Planck scale interactions. In this case, reheating to the intermediate scale after inflation would give f_X^o in the desired range.

3

Our analysis does not apply to the case that the X carries negative baryon number and is light enough that the average anti-nucleon to nucleon ratio of the decay products is an order of magnitude or more.

The allowed ranges of M_X and f_X^o are correlated such that

$$\frac{f_X^o}{f_B}\frac{M_X}{100GeV} \sim \mathcal{O}(1).$$

When this is combined with the allowed values for τ_X , it is apparent that the X particles never dominate the energy density of the universe. The universe is still radiation dominated at the era of X decay. Hence the time-temperature relation during this era is given by:

$$(\frac{t}{10^6 sec}) \simeq 1.32(\frac{keV}{T})^2 \tag{2.1}$$

and X decays occur in the keV era.

We ignore the possibility that X has totally invisible decays, for example into neutrinos. Decays to neutrinos are invisible in the sense that, for the τ_X and M_X of interest, the probability of a decay neutrino interacting in the hot plasma is extremely small.[4] If such totally invisible decays occur, our results still apply but

---

4

The few neutrinos which do interact in the plasma can alter the light element abundances. For neutrinos and anti-neutrinos of sufficiently low energy that neutrino-nucleon scattering cannot produce pions, the dominant processes are $\bar{\nu}p \rightarrow e^+n$ and $\nu n \rightarrow ep$. The former produces neutrons, some of which become deuterium via $np \rightarrow d\gamma$, and the latter depletes ^4He, since the vast majority of neutrons present at the keV era are in ^4He. For the ranges of X parameters of interest to us, these abundance modifications are negligible. However, $\Omega_B = 1$ scenarios can be constructed where D and ^4He abundances are substantially adjusted by neutrino reactions. We do not pursue these here, since the ^7Li overabundance is not addressed by this mechanism.

with f_X^o appropriately increased. We also assume that there is no missing energy in the electromagnetic and baryonic decays. If some energy is lost from the hot plasma, for example in neutrinos, then our analysis and results still apply, but with proper rescaling of M_X, r_B and f_X^o.

3. Observations

Unlike many other fields in modern cosmology, there exists a wealth of data with which to test our theoretical understanding of the primordial synthesis of the light elements. Since the early qualitative successes of Big Bang nucleosynthesis (Wagoner,Fowler and Hoyle 1967: Wagoner 1967; Wagoner 1968), astronomers have attempted to determine more accurately the primordial light element abundances. Besides the considerable observational difficulties in measuring precisely the very small fractional abundances involved, the great challenge of this programme has been to correctly relate the measured abundances to actual primordial abundances. In this chapter we briefly summarize the current status of the field as it pertains to this work.

3.1. DEUTERIUM

Deuterium is detected mostly through the isotopic shift of lines of atomic H I and deuterated molecules. This approach has been used in stellar atmospheres, in the interstellar gas and in planetary atmospheres. Stellar D has not been detected, though upper limits have been obtained. A conservative limit is $D/H < 10^{-6}$ (Boesgaard and Steigman 1985). Deuterium in the interstellar medium has been detected in the Lyman lines of H I along the line of sight to nearby cool stars and to more distant O and B stars; however, stellar contamination of the interstellar profile, multiple clouds in the line of sight, and high velocity "puffs" of stellar H I complicate the derivation of the interstellar D/H values (Vidal-Madjar et al 1983; Gry et al 1983; Gry et al 1984). Boesgaard and Steigman take the most probable interstellar D/H value to be $0.8 - 2.0 \times 10^{-5}$, although Vidal-Madjar et al claim that $5 \times 10^{-6} - 5 \times 10^{-5}$ is consistent with observations (Vidal-

Madjar et al 1983) and some-authors have quoted values as low as 2.4×10^{-6} along the line of sight toward nearby cool stars (Dupree et al 1977). Voyager I observations of deuterated molecules in the Jovian troposphere yield a D/H range of $1.2 - 3.1 \times 10^{-5}$ (Encrenaz and Combes 1982). Some authors (Hubbard and MacFarlane 1980) argue that the amount of D present in the atmospheres of Jupiter and Saturn will be close to the presolar value, while others believe that chemical fractionation and other enhancement processes may have significantly affected its abundance.

To determine the primordial abundance of deuterium requires both an accurate determination of the current abundance and a complete theoretical understanding of evolution of the abundance to the present day. During the chemical evolution of the galaxy any primordial D which is processed through stars is completely destroyed. The efficiency of processing depends on the birth rate function, the initial mass function, mass loss rates, infall to and mixing in the galactic disk, etc. Various models suggest that astration is 50% to $>$ 90% efficient, so the present abundance of D could be $1/2- < 1/20$ of its primordial value (for example Pagel 1982).

We take as our range for the post-astration abundance of deuterium 5.0×10^{-6} to 5.0×10^{-5}.

3.2. HELIUM-3

As stated by Boesgaard and Steigman the value of ^3He as a probe of primordial nucleosynthesis is very unclear at present (also R. Wagoner private communication, A.M. Boesgaard private communication). Since ^3He can be both destroyed and produced (by conversion of D and by incomplete H burning) in

stars, the present abundance could be much greater or much less than the primordial abundance. The situation is exacerbated by the wide range in the observed abundance. Presolar abundances inferred from measurements on meteorites and the solar wind are approximately $1 - 2 \times 10^{-5}$ (Boesgaard and Steigman 1985), while observations of H II regions yield a wide range of values as high as 1.5×10^{-4}, with no apparent correlation with any physical parameters (Rood et al 1984; Bania et al, as communicated by Boesgaard) Such a range of ^3He abundances may be difficult to account for by stellar processing of the solar system abundances. The pre-Pop I average ^3He abundance could be significantly greater than the solar system value.

We adopt as our maximum range for the pre-Pop I average ^3He abundance $1 \times 10^{-5} - 1.5 \times 10^{-4}$.

3.3. HELIUM-4

According to Boesgaard and Steigman the best value for the primordial helium mass fraction Y_p comes from isolated extragalactic H II regions. Combined results from various authors give $Y_p = 0.245 \pm 0.003$ (Kunth 1983). More recently Steigman, Gallagher and Schramm (1987) reported 0.235 ± 0.012, while Pagel (1987) has quoted 0.22. The actual value will not be of great significance for our work, except to affect, in an easily computed fashion, the allowed branching ratio and abundance of the X, and the range of permitted pre-keV nucleosynthesis scenarios.

3.4. LITHIUM

The ^7Li abundance observed in stars varies over a wide range. ^7Li is produced by spallation and can be destroyed in stellar regions which are hotter than about 2.5×10^6 $^\circ K$ by the reaction $^7Li(p,\alpha)^4He$. The timescale on which ^7Li is destroyed in a region of a star is a strong function of the temperature of that region: 10^6 years for $T = 3.5 \times 10^6$ $^\circ K$ and 10^{11} years for $T = 2.0 \times 10^6$ $^\circ K$ (Maurice et al 1984). The depths to which ^7Li is circulated from the surface depends on various properties of the star, such as its effective temperature T_e, and hence different stars have different depletions of surface ^7Li. In many population I stars, such as the sun, this has led to significant depletion of ^7Li over the lifetime of the star.

It has been argued that the ^7Li abundance seen in many low metallicity, halo dwarf, population II stars reflects the true primordial abundance (Spite and Spite 1982). The evidence for this claim is that, for $5500^\circ < T_{eff} < 6300^\circ$, the ^7Li abundance is constant (at $\simeq 10^{-10}$ the hydrogen abundance), suggesting that little ^7Li depletion has occurred in any of these stars. For $T_{eff} < 5500^\circ$ the ^7Li abundance drops sharply.

It is known from studies of the spectral lineshape that the lithium seen in these old stars is predominantly ^7Li and not ^6Li (Maurice et al 1984). Although ^6Li has not been seen in these stars, it could be there at a 10% level compared with ^7Li.

^6Li is destroyed in stars by the process $^6Li(p,^3He)^4He$. At any given temperature, this occurs with a cross-section almost 100 times that of ^7Li destruction. Hence a star with even mild ^7Li depletion can have very large ^6Li depletion, depending on the fraction of surface material convected to regions of sufficiently

high temperature. In the dwarf halo stars studied by Spite and Spite (1982), where little ^7Li depletion is argued to have occurred, a large depletion of ^6Li is probable. According to one theoretical analysis of the ^7Li data of these stars (Rebolo et al 1986) the surface material must be convected and diffused down to a temperature of $T = 2.3 \times 10^6 \ ^\circ K$ for all these stars (independent of T_e). In this case essentially all the ^6Li of these stars would be destroyed.

Another possibility is that ^6Li will be efficiently destroyed in the protostellar phase, if the protostar is fully convective at a high enough temperature (D.Bond, L.Nelson, D.Vandenberg in preparation).

The observed ^7Li abundance in Population I is $\mathcal{O}(10^{-9})$; this is higher than the 10^{-10} seen in Population II. This suggests that the ^7Li abundance in the disk has been enriched.

There is also a reported limit of $^6Li/^7Li < 1/10$ in the ISM along the lines of sight toward two stars (Snell et al, 1981). This may or may not represent the primordial ratio depending on the history of the intervening gas. The chemical evolution of the disk depends on the amount of galactic astration. It is a reasonable assumption that ^6Li is destroyed in the astrated matter (Audouze et al 1983). With this in mind we consider a maximum range for the primordial ^7Li abundance to be 5×10^{-11} to 5×10^{-9}.

4. Physics of the KeV Era

When a particle of mass greater than a few GeV decays during the keV era, some of the energy goes into elecromagnetic decay products, and some goes into hadrons. Both classes of decay products form showers as they thermalize with the background plasma. In this chapter we examine the development of these showers and write down the resulting dynamical equations for the abundances of the light elements.

4.1. Electromagnetic Showers

When a massive X decays electromagnetically or hadronically, it injects very energetic photons, electrons and positrons into the relatively cool ($T = 1 - 30$ kev) background plasma. In thermalizing with the background, these energetic particles create showers. Burns and Lovelace (1982) and Aharonian and Vardanian (1985) studied relativistic electron-photon shower production in a plasma. They found that when energetic photons are injected into a gas of monochromatic photons of energy E_o, the dominant mechanism for photon energy loss is $e^+ - e^-$ pair production. This has a kinematic threshold $E_{th} = m_e^2/T$. The resulting shower electrons, lose energy chiefly through inverse Compton scattering off background photons. After several pair-production mean free paths, the remaining photons are below the pair-production threshold and are found to have the energy spectrum

$$\xi_\gamma(E) \sim \begin{cases} E^{-\frac{3}{2}} & 0 \leq E \leq E_{th} \\ 0 & E_{th} \leq E \ . \end{cases} \tag{4.1}$$

These post pair-production photons are called "breakout" photons. In the ab-

sence of ambient charged particles, and neglecting Delbruck scaterring, the photon spectrum would not evolve further.

The background photons are not monoenergetic, they have a thermal distribution with temperature T. Energetic photons can pair produce off ambient photons in the tail of the thermal distribution. This lowers the threshold energy. The primordial plasma, however, also contains electrons and protons , with $f_p \equiv n_p/n_\gamma = 2.8\ 10^{-8}\Omega_B h_o^2$, and $f_p = f_e$ by charge neutrality ($T \ll m_e$) . The energetic photons can therefore lose energy by Compton scattering, mostly off background electrons. The shower evolution is continued until Compton scattering becomes comparable to the pair production process for the most energetic photons of the shower. At this point the most energetic shower photons have energy $E_{max} \sim m_e^2/25T$. From then on, we evolve the photon distribution using the now dominant Compton scattering and photo-dissociation, as described later. Note that E_{max} is time dependent and monotonically increasing. As E_{max} surpasses the photodissociation thresholds of the various elements, more and more tightly bound species become susceptible to photo-destruction (cf. fig.1). Since E_{max} depends on the interplay between Compton scattering and pair production, it depends on $\Omega_B h_o^2$. This dependence is weak and has only a slight effect on our results.

We now discuss the normalization of the photon spectrum. If X does not carry baryon number, or if $M_X \gg$ 1GeV, the average hadronic jet has only $\sim$ 10% of its energy in the form of baryons. Hence, decay baryons carry off only a small fraction of M_X. Ignoring energy loss to neutrinos, we therefore normalize the break out spectrum to have total energy M_X. Defining $\xi_\gamma(E)dE$ to be the

number of breakout photons of energy E produced per X decay, we take[5]

$$\xi_\gamma(E) = \begin{cases} \frac{M_X}{2E_{max}^{1/2}} E^{-3/2} & 0 \leq E \leq E_{max} \\ 0 & E_{max} \leq E \ , \end{cases} \tag{4.2}$$

which is plotted in fig. 2. These photons are responsible for the photo-dissociation of the light elements.

4.2. SHOWERS CONTAINING PRIMARY BARYONS

When an X decays, it has some branching ratio r_B to produce baryons . The average number of baryons produced in a hadronic X decay can be deduced from $e^+ - e^-$ jet data (Schwitters 1983) at $E_{cm} = M_X$. For $M_X = 1\text{TeV}$, there are on average about five nucleon-antinucleon pairs, with ~ 5 GeV energy per nucleon, and even smaller values as $M_X \rightarrow 1GeV$. The multiplicity is logarithmically dependent on E_{cm}. We take the average numbers of jet protons and jet neutrons to be equal.

As a proton moves through the background plasma, it can lose energy by bremsstrahlung off background protons or electrons, synchrotron radiation, inverse Compton scattering off thermal photons Coulomb scattering off background electrons and plasmon excitations and strong interactions. At kinetic energies greater than ~ 1 GeV the dominant energy loss mechanism is strong interactions; below 1 GeV Coulomb scattering and excitation of plasma oscillations dominate

---

5

Although this power law may be altered by the inclusion of Delbruck or by the averaging over the thermal photon distribution, our results are relatively insensitive to the exact shape of the spectrum.

(though the rate for inverse Compton scattering is large, the energy transfer is small). Neutrons lose energy only through strong interactions.

While strong interactions dominate their energy loss, the energetic baryons scatter many times off background protons and alpha particles, producing several energetic d,^3H,^3He and ^4He, and destroying some of the background alphas. Even as these energetic light nuclei lose energy by Coulomb scattering, they can collide with background alphas producing ^6Li,^7Li and ^7Be. Eventually the remaining energetic baryons thermalize and join the sea.

We proceed to calculate ξ_i, the number of nuclear species i produced per X decay. Let

$$ {}_rP_a^{j_a}(E_r) = \frac{n_a \sigma^{j_a}(E_r)}{\sum_b \sum_{k_b} n_b \sigma^{k_b}(E_r)} \tag{4.3} $$

be the probability that a baryon r ($r = n, p$) of energy E_r, scatters off a nuclear species a ($a = p, \alpha$) via reaction j_a, where j_a runs over the reactions in table (Table 1). Let $\vartheta_m^{j_a}(E_r, E_m)$ be the number of species m produced with energy E_m per reaction j_a at baryon energy E. Then

$$ {}_rg_m(E_r, E_m) = \sum_a \sum_{j_a} {}_rP_a^{j_a}(E_r) \vartheta_m^{j_a}(E_r, E_m) \tag{4.4} $$

is the average number of species m of energy E_m produced by a baryon r of energy E_r in one baryon collision.

For example, consider a 5 GeV neutron (cf Fig. 3). The number density of alpha particles is one-tenth the number density of protons. The total neutron-alpha cross section at 5 GeV is 130 mb. The total neutron-proton cross section is 41 mb. Therefore the probability of scattering off a proton is 75%, and off an alpha is 25%. The inelastic neutron-alpha cross section at 5 GeV is 100 mb;

of that 30 mb is $n\alpha \longrightarrow dpnn$, and 11 mb is $n\alpha \longrightarrow ddn$. Therefore

${}_nP_\alpha^{n\alpha\to dpnn} = 0.25 \times \frac{100}{130} \times \frac{30}{100} = 0.06$

and

${}_nP_\alpha^{n\alpha\to ddn} = 0.25 \times \frac{100}{130} \times \frac{11}{100} = 0.02.$

Thus

${}_ng_d = 0.06 + 2 \times 0.02 = 0.10.$

It is essential to include secondary baryons in the shower calculations. For large initial baryon energy ($\gtrsim$ 1 GeV) there are three classes of secondary baryons: a) baryons which have elastically scattered, retaining almost all of their initial energy; b) baryons which have inelastically scattered, losing a fraction $1 - \epsilon$ of their initial energy; c) debris baryons which are the old target protons or parts of the target alphas; these have energies of approximately 50 to 200 MeV. Unfortunately ϵ is not well determined in the energy range of interest. It is taken to be (Bucza, private communication) between 40% and 75%. At lower energies these classes become less distinct. Neutrons must be traced down to $\sim$ 25 MeV where the elastic neutron-proton cross section dominates all other processes. Protons must be traced to $\sim$ 1 GeV below which they rapidly lose energy by Coulomb scattering and plasmon excitations.

To obtain the ξ_i's, we must sum the contributions of all secondary, tertiary, etc. baryons, average over the neutron and proton contributions, and multiply by the baryon multiplicity:

$$\xi_m = \nu_B \times \frac{1}{2} \sum_{r=n,p} \sum_{E_m} \sum_{E_{p\prime}, E_{p\prime\prime}, \cdots > 1GeV} \sum_{E_{n\prime}, E_{n\prime\prime}, \cdots > 25MeV}$$

$$\{{}_rg_m(E_{in}, E_m) + {}_r\, g_{n\prime}(E_{in}, E_{n\prime})[{}_{n\prime}g_m(E_{n\prime}, E_m) + \qquad (4.5)$$

$$+_{n\prime}g_{n\prime\prime}(E_{n\prime},E_{n\prime\prime})(_{n\prime\prime}g_m(E_{n\prime\prime},E_m)+\cdots)+_{n\prime}g_{p\prime\prime}(_{p\prime\prime}g_m+\cdots)]+$$

$$+_r g_{p\prime}[_{p\prime}g_{n\prime\prime}(_{n\prime\prime}g_m+\cdots)+_{p\prime}g_{p\prime\prime}(_{p\prime\prime}g_m+\cdots)]\}$$

We have taken the initial energies, E_{in}, of the primary baryons to be 5 GeV, and the baryon multiplicity, ν_B, to be 5, which are their values at $M_X = 1$TeV. As discussed in section 4.3, the dependence of these quantities on M_X is partly into the baryonic branching ratio r_B.

Using the procedure outlined above, we calculate ξ_d,$\xi_{^3H}$, $\xi_{^3He}$, and ξ_n, respectively the average number of deuterons, tritons, ^3He nuclei, and $\sim$ 25 MeV neutrons, produced per X decay; $\xi_{^4He}$, the average number of alpha particles scattered out of the thermal sea to MeV energies; and ξ_α^K, the number of alpha particles destroyed. The results are listed in Table 2. All the cross-sections and other data necessary for the determination of the ξ's are found in Table 3.

A posteori, the values of these ξ's can be easily understood. For $\epsilon = 0.25$, a 5 GeV nucleon takes approximately eight scatterings to fall below 500 MeV, producing two or three 200 MeV neutrons en route. These 200 MeV neutrons scatter two or three more times before falling below the threshold for helium-4 destruction. Thus, about fifteen scatterings occur in all. One quarter of these are off background α's, and three quarters of those break up ^4He. For five 5 GeV nucleons we therefore expect about $15 \times 1/4 \times 3/4 \times 5 = 15$ ^4He's to be destroyed. In case of a ^4He breakup, the cross sections for single ^3He, ^3H and D production are approximately equal. However, there is also a two deutron channel and, for low energy neutrons, a ^3Hd channel. We therefore expect more deuterium than tritium, and more tritium than helium-3, in agreement with the calculated values, $\xi_2 = 7, \xi_{^3H} = 6$ and $\xi_{^3He} = 4$. One quarter of nucleon alpha

scatterings are elastic, we therefore expect $15 \times 1/4 \times 1/4 \times 5 = 5$ energetic α's, close to the calculated value of seven.

The calculation of $\xi_{^6Li}$, $\xi_{^7Li}$ and $\xi_{^7Be}$ involves the spectra of energetic ^3H, ^3He, and ^4He produced in the baryon shower. For example, the dominant production mechanism for ^6Li is $t\alpha \rightarrow n^6Li$. The probability that a tritium of energy E'' interact with an α and produce a ^6Li while traveling a distance dx is

$$n_\alpha \sigma_{\alpha t \rightarrow n^6 Li}(E'')dx;$$

so the probability that a tritium of energy E' produce a ^6Li while losing energy electromagnetically to the background plasma is

$$\int_0^{E'} n_\alpha \sigma_{\alpha t \rightarrow n^6 Li}(E'')(\frac{dx}{dE})|_{E''} dE''.$$

dE/dx is the Coulomb and plasmon energy loss of a triton. This is calculated using formula (13.88) of Jackson (Jackson 1975)

$$\frac{dE}{dx} = \frac{Z^2\alpha}{v^2}\omega_p^2 \ln(\frac{\Lambda v}{\omega_p b_{min}}), \tag{4.6}$$

with

$$b_{min} = max(\frac{1}{\gamma m v}, \frac{\alpha}{\gamma m v^2}),$$

$$\omega_p^2 = \frac{4\pi n \alpha}{m}$$

and $\Lambda = \mathcal{O}(1)$. The probability that a triton produced in a $N - \alpha$ collision have

energy E' is

$$\frac{1}{\sigma_{N\alpha\to t+\cdots}}\left(\frac{d\sigma_{N\alpha\to t+\cdots}}{dE_t}\right)_{E'}.$$

This is taken to be independent of the incoming nucleon energy over the energy range of interest (Meyer 1972). Finally, the ^6Li yield is

$$\xi_{^6Li} = (\xi_t + \frac{1}{4}\xi_{^3He}) \times \int_0^\infty \frac{1}{\sigma_{N\alpha\to t+\cdots}}\left(\frac{d\sigma_{N\alpha\to t+\cdots}}{dE_t}\right)_{E'} \times \int_0^{E'} n_\alpha \sigma_{\alpha t\to n^6Li}(E'')\left(\frac{dx}{dE}\right)|_{E''}dE''dE', \quad (4.7)$$

where we have assumed that $\sigma(N\alpha\to t+\cdots) = \sigma(N\alpha\to{}^3He+\cdots)$ and $\sigma(\alpha t \to n^6Li) = \sigma(\alpha^3He \to p^6Li)$. The factor of $1/4$ for $\xi_{^3He}$ is due to the $1/Z^2$ in the Coulomb loss formula. This gives $\xi_{^6Li} \approx 3-7\ \ 10^{-5}$.

The calculation of $\xi_{^7Li}$ and $\xi_{^7Be}$ is similar to that of $\xi_{^6Li}$. The dominant production reactions are $\alpha^\star\alpha\to p^7Li$ and $\alpha^\star\alpha\to n^7Be$, with $\alpha^\star$ coming from $N-\alpha$ elastic scattering. However, the spectrum of the energetic alphas depends on the incident nucleon energy. We therefore calculate the probability $P^{el}(E_N)$ that a nucleon of energy E_N , having undergone an elastic collision with a background α, result in production of an ^7Li (or ^7Be),

$$P^{el}(E_N) = \int_0^\infty \frac{1}{\sigma^{el}_{N\alpha}}\left(\frac{d\sigma^{el}_{N\alpha}}{dE_t}\right)_{E'} \int_0^{E'} n_\alpha \sigma_{\alpha\alpha\to p^7Li}(E'')\left(\frac{dx}{dE}\right)|_{E''}dE''dE', \quad (4.8)$$

and sum over all such elastic collisions in the shower. This yields $\xi_{^7Li} \approx 1-2.5\ \ 10^{-6}$ and $\xi_{^7Be} \approx 1-2.5\ \ 10^{-6}$.

The ratio of $\xi_{^6Li}$ to $\xi_{^7Li}$ is easily understood. Energetic α's which produce lithium-7 lose energy a factor of $Z^2 = 4$ faster than the tritons producing lithium-6. Also the average production cross section of ^6Li is a factor of five larger than that of ^7Li. Since the yield of energetic α's is approximately equal to the number of energetic tritons, we expect twenty times more lithium-6 than lithium-7.

Equipped with these yields we can write down the equations governing the abundances of the light elements during the period of X decay, and solve them.

4.3. Effective Baryonic Branching Ratio

In calculating the baryon shower yields, ξ_i, we took the baryon multiplicity and the primary baryon energy for $M_X = 1$ TeV; $\nu_B = 5$ and $E_{in} = 5$ GeV (Schwitters 1983) The number and the energy of the primary baryons actually depends on the mass of the X. For other values of the X mass, ν_B depends logarithmically on the energy, except near the baryon production threshold where the dependence is stronger. The value of ν_B, however, can be absorbed into an effective baryonic branching ratio,

$$r_B^* = r_B \frac{\nu_B}{5} \mathcal{F}.$$

Here r_B is the true baryonic branching ratio, and $\mathcal{F}$ is a factor which represents the dependence of the yields, ξ's, on the energy of the primary shower baryons. For instance, if a shower consists of five 1 GeV baryons, a similar analysis to the last section would give us new values for the ξ's, $\xi_d(1GeV) = 0.35\xi_d(5GeV)$, $\xi_{^3H}(1) = 0.4\xi_{^3H}(5)$, $\xi_{^3He}(1) = 0.4\xi_{^3He}(5)$, $\xi_{^7Li}(1) = 0.5\xi_{^7Li}(5)$ and $\xi_\alpha^K(1) = 0.35\xi_\alpha^K(5)$. Therefore $\mathcal{F} \sim 0.4$.

Working with r_B^* instead of r_B allows us to consistently use the same values for the ξ's as given for a 1 TeV X particle. To compute the true value of the baryonic branching ratio r_B, one needs $\nu_B \times \mathcal{F}/5$ as a function of the X mass. It is worth mentioning that $\xi_{^7Li}$ scales slightly differently than the other ξ's as a function of the primary baryon energy for low M_X. For example, we have $\xi_{^3He}(1GeV) = 0.4\xi_{^3He}(5GeV)$,while $\xi_{^7Li}(1GeV) = 0.5\xi_{^7Li}(5GeV)$. We have ignored this difference. This means that for $M_X < 1$ TeV, the true ^7Li abundance may be higher than our result by a factor of $\sim 0.5/0.4$. Similarly, for $M_X \gg$ 1TeV, the ^7Li abundance may be slightly lower than indicated.

4.4. REACTIONS

Let f_i be the reduced number density of species i, the number density divided by the number density of thermal photons, $n_{\gamma_{th}}$. The equations governing the light element abundances are:

$$\begin{aligned} \dot{f}_{\gamma^*}(E) = & \xi_{\gamma^*}(E) f_X^o \Gamma_X e^{-t/\tau_X} \\ & + f_p f_n n_{\gamma_{th}} c \frac{d\sigma_{nA\to A'\gamma}}{dE_\gamma} \\ & - f_{\gamma^*}(E) n_{\gamma_{th}} c (f_e \sigma_C + f_d c \sigma^D_{A\gamma}(E)) \end{aligned} \tag{4.9}$$

$$\begin{aligned}
\dot{f}_n &= r_B^* \xi_n f_X^o \Gamma_X e^{-t/\tau_X} \\
&+ n_{\gamma_{th}} c \int_0^{E_{max}} f_{\gamma^*}(E) \sum_A g_A(E) f_A \sigma_{\gamma A}^D dE \\
&- f_n n_{\gamma_{th}} (f_p (\sigma v)_{np \to d\gamma} + f_d (\sigma v)_{nd \to {}^3H\gamma} + \\
&\qquad f_{^3He}((\sigma v)_{n^3He \to {}^3Hp} + (\sigma v)_{n^3He \to \alpha\gamma}) + \\
&\qquad + f_{^6Li}((\sigma v)_{n^6Li \to \alpha^3H} + (\sigma v)_{n^6Li \to \gamma^7Li}) + \\
&\qquad + f_{^7Li}(\sigma v)_{n^7Li \to \gamma^8Li} + f_{^7Be}(\sigma v)_{n^7Be \to p^7Li}) \\
&- f_n \Gamma_n
\end{aligned} \tag{4.10}$$

$$\begin{aligned}
\dot{f}_d &= r_B^* \xi_d f_X^o \Gamma_X e^{-t/\tau_X} + f_p f_n n_{\gamma_{th}} (\sigma v)_{np \to d\gamma} \\
&+ n_{\gamma_{th}} c \int_0^{E_{max}} f_{\gamma^*}(E) (f_\alpha \sigma_{\gamma\alpha \to d+\cdots}(E) + f_{^3H} \sigma_{\gamma^3H \to d+n}(E) \\
&\qquad + f_{^3He} \sigma_{\gamma^3He \to d+p}(E)) dE \\
&- f_d n_{\gamma_{th}} (f_n (\sigma v)_{nd \to {}^3H\gamma} + \int_0^{E_{max}} f_{\gamma^*}(E) c \sigma_{d\gamma}^D(E) dE)
\end{aligned} \tag{4.11}$$

$$\begin{aligned}
\dot{f}_{^3H} &= r_B^* \xi_{^3H} f_X^o \Gamma_X e^{-t/\tau_X} \\
&+ f_n n_{\gamma_{th}} (f_{^3He} (\sigma v)_{n^3He \to {}^3Hp} + f_{^6Li} (\sigma v)_{n^6Li \to {}^3H\alpha} + f_d (\sigma v)_{nd \to {}^3H\gamma}) \\
&+ f_\alpha n_{\gamma_{th}} c \int_0^{E_{max}} f_{\gamma^*}(E) \sigma_{\alpha\gamma \to {}^3H+\cdots}(E) dE \\
&- f_{^3H} n_{\gamma_{th}} c \int_0^{E_{max}} f_{\gamma^*}(E) \sigma_{^3H\gamma}^D(E) dE - r_B^* \frac{4}{5} \xi_{^6Li} f_X^o \Gamma_X e^{-t/\tau_X}
\end{aligned} \tag{4.12}$$

$$\dot{f}_{^3He} = r_B^* \xi_{^3He} f_X^o \Gamma_X e^{-t/\tau_X}$$
$$+ f_\alpha n_{\gamma_{th}} c \int_0^{E_{max}} f_{\gamma^*}(E) \sigma_{\alpha\gamma \to {}^3He + \ldots}(E) dE \tag{4.13}$$
$$- f_{^3He} n_{\gamma_{th}} \left(\int_0^{E_{max}} f_{\gamma^*}(E) c \sigma^D_{^3He\gamma}(E) dE + f_n (\sigma v)_{n^3He \to p^3H} \right)$$
$$- r_B^* \frac{1}{5} \xi_{^6Li} f_X^o \Gamma_X e^{-t/\tau_X}$$

$$\dot{f}_\alpha = -r_B^* \xi_\alpha^K f_X^o \Gamma_X e^{-t/\tau_X} - r_B^* (\xi_{^7Li} + \xi_{^7Be}) f_X^o \Gamma_X e^{-t/\tau_X}$$
$$- f_\alpha n_{\gamma_{th}} c \int_0^{E_{max}} f_{\gamma^*}(E) \sigma^D_{\gamma\alpha}(E) dE \tag{4.14}$$

$$\dot{f}_{^6Li} = r_B^* \xi_{^6Li} f_X^o \Gamma_X e^{-t/\tau_X}$$
$$+ n_{\gamma_{th}} c \int_0^{E_{max}} f_{\gamma^*}(E) (f_{^7Li} \sigma_{\gamma^7Li \to n^6Li}(E) + f_{^7Be} \sigma_{\gamma^7Be \to p^6Li}(E)) dE \tag{4.15}$$
$$- f_{^6Li} n_{\gamma_{th}} \left(\int_0^{E_{max}} f_{\gamma^*}(E) c \sigma^D_{\gamma^6Li}(E) dE + f_n (\sigma v)_{n^6Li \to t\alpha} \right)$$

$$\dot{f}_{^7Li} = r_B^* \xi_{^7Li} f_X^o \Gamma_X e^{-t/\tau_X}$$
$$+ f_n f_{^7Be} n_{\gamma_{th}} (\sigma v)_{n^7Be \to p^7Li} + f_{^7Be} \Gamma_{^7Be} + \tag{4.16}$$
$$- f_{^7Li} n_{\gamma_{th}} \left(\int_0^{E_{max}} f_{\gamma^*}(E) c \sigma^D_{\gamma^7Li}(E) dE + f_n (\sigma v)_{n^7Li \to \gamma^8Li} \right)$$

$$\dot{f}_{^7Be} = r_B^* \xi_{^7Be} f_X^o \Gamma_X e^{-t/\tau_X}$$
$$- f_{^7Be} n_{\gamma_{th}} (f_n (\sigma v)_{n^7Be \to p^7Li} + \int_0^{E_{max}} f_{\gamma^*}(E) c \sigma^D_{\gamma^7Be}(E) dE \qquad (4.17)$$
$$- f_{^7Be} \Gamma_{^7Be},$$

where σ_C is the Compton cross section, σ^D 's are photodissociation cross sections, $g_A(E)$ is the mean number of neutrons produced by photodissociation of nucleide A by a photon of energy E, and f_X^o is the number density of X's divided by the number density of thermal photons, after the x's fall out of thermal equilibrium. In the photon equation, $f_{\gamma^*}(E)$ represents the reduced number density of photons with energy between E and E+dE, and A and A' represent any light nuclei. These equations are represented diagrammatically in Fig. 4.

Many of the terms in the above equations can be ignored. In the photon equation, since $\dot{\xi}_\gamma \equiv \int_0^\infty \xi_\gamma(E) dE$ is much greater than ξ_n, the only important source of energetic photons is direct production from X decays. Also, because the number density of electrons, f_e, is much greater than the number densities of the light elements, and because the Compton cross-section is large compared to photo-dissociation cross-sections, the only important sink of energetic photons is Compton scattering off electrons. The photon equation is now

$$\dot{f}_{\gamma^*}(E) = \xi_{\gamma^*}(E) f_X^o \Gamma_X e^{-t/\tau_X} - f_{\gamma^*}(E) f_e n_{\gamma_{th}} c \sigma_C(E). \qquad (4.18)$$

The photon equation decouples from the rest, greatly simplifying both the analytic and numerical solutions. Note that, when E_{max} is less than the threshold energy, Q, for a particular photo-reaction, then $\int_0^{E_{max}} f_{\gamma^*}(E) \sigma(E) dE$ is equal to zero because of the threshold in the source term ξ_{γ^*} ; thus, there is an effective theta function in time in all photo-reaction terms.

In the neutron equation, the neutrons were taken to be thermal. Thermalization is brought about by n-p elastic scattering, which dominates all other reactions, including decay. ξ_n, which had been calculated to be the yield of $\sim$ 25MeV neutrons per X decay, was therefore taken to be the yield of thermal neutrons. As a neutron sink, neutron capture by the mass six and seven elements, can be ignored because of these elements' low abundnaces. Neutron capture by deuterium, and $n^3He \rightarrow \alpha\gamma$ are electromagnetic, and hence suppressed. With these modifications, the neutron equation is

$$\begin{aligned} \dot{f}_n = & r_B^* \xi_n f_X^o \Gamma_X e^{-t/\tau_X} \\ & - f_n n_{\gamma_{th}} (f_p (\sigma v)_{np \rightarrow d\gamma} + f_{^3He} ((\sigma v)_{n^3He \rightarrow ^3Hp}) \\ & - f_n \Gamma_n . \end{aligned} \tag{4.19}$$

Unfortunately, $n^3He \rightarrow p^3H$ cannot be ignored at early times so the neutron equation remains coupled to the ^3He equation. We did drop photodissociation of the light elements as a source of neutrons. As the various elements become vulnerable, they contribute to an effective ξ_n which is up to a factor of three larger than the tabulated value. However, ex post facto we find that the final element abundances are only noticeably affected if ξ_n is increased by a factor of approximately 100.

Several other terms were dropped from the equations. $n^6Li \rightarrow \alpha^3H$ was neglected as a source of ^3H because ^6Li abundances are very small. Similarly, $\alpha^3H \rightarrow n^6Li$, $\alpha^3He \rightarrow p^6Li$ and $\alpha\alpha \rightarrow p^7Li$ were ignored as depletion mechanisms for ^3H, ^3He and ^4He respectively since so little ^6Li and ^7Li were produced, ie

$\xi_{^6Li} \ll \xi_{^3H}, \xi_{^3He}$ and $\xi_{^7Li} \ll \xi_\alpha^K$. The new ^3H equation is

$$\begin{aligned}\dot{f}_{^3H} &= r_B^* \xi_{^3H} f_X^o \Gamma_X e^{-t/\tau_X} \\ &+ f_n n_{\gamma_{th}} f_{^3He} (\sigma v)_{n^3He \to {}^3Hp} \\ &+ f_\alpha n_{\gamma_{th}} c \int_0^{E_{max}} f_{\gamma^*}(E) \sigma_{\alpha\gamma \to {}^3H + \cdots}(E) dE + \\ &- f_{^3H} n_{\gamma_{th}} c \int_0^{E_{max}} f_{\gamma^*}(E) \sigma^D_{^3H\gamma}(E) dE.\end{aligned} \tag{4.20}$$

with similar modifications to the ^3He and α equations.

We have now reached the point where we can discuss both the analytic and numerical solutions to these equations and demonstrate the existence of $\Omega_B = 1$ scenarios which are not in conflict with the primordial abundances of the light elements inferred from observations.

4.5. UNCERTAINTIES

Although we were as careful as possible, there are several sources of uncertainty in our calculation which we were unable to avoid. For certain quantities no data was available; for others, the existing data was incomplete, contradictory, or had large experimental errors. Many of these translate into uncertainties in the paramters M_X, r_B^*, and (f_X^o/f_p) ; thus, they would only be of relevance if we cared to precisely determine the properties of the X particle. However, some of the uncertainties in the data imply uncertainties in the ratios of the ξ's. It is crucial to keep this in mind since a favourable alteration in the ξ_i ratios would widen the allowed parameter space for the X, while an unfavourable alteration

could close it entirely. Improved values for the ξ_i's will require new experimental data followed by Monte Carlo studies of the baryonic showers.

From our results it will become clear that the most important sources of uncertainty are in the determinations of ξ_7 and $\xi_{^6Li}$. For ^7Li, the dominant production mechanism is $\alpha^*\alpha \rightarrow p^7Li$; for ^7Be, it is $\alpha^*\alpha \rightarrow n^7Be$. Here α^* is an energetic alpha particle produced in elastic $N-\alpha$ scattering. Because the cross-section for $\alpha\alpha \rightarrow 7$ falls exponentially as a function of E_α, ξ_7 is very sensitive to the energy distribution of the α^*'s. Unfortunately, we could not find $d\sigma/dE_\alpha$ for $N-\alpha$ elastic scattering above $E_{lab} \sim 2$GeV (Klem et al 1977; Meyer 1972). We took $\sigma^{-1}(d\sigma/dE_\alpha)$ to be constant for nucleon energies above 1.78 GeV, since it is the same for 800 MeV to 1.78 GeV. We were also unable to find any data on the photo-dissociation of ^7Be. We assumed that the photo-dissociation cross-sections of ^7Be is equal to the cross-section for ^7Li because they are image nuclei. One might expect a lower threshold for ^7Be than for ^7Li because of the greater Coulomb energy. This would mean a very slightly lower abundance of mass seven elements than we report, since more ^7Be would be destroyed.

For ^6Li, the dominant production mechanism is $^3H^*\alpha \rightarrow n^6Li$. The energetic ^3H's are produced in $p-\alpha$ inelastic scattering. We could find data on $d\sigma^{p\alpha \rightarrow t}/d\Omega$ only for $E_p^{lab} = 90, 300$MeV (Meyer 1972). Since it was identical for those two energies, we assumed it was the same for all the E_p of interest. The justification for this is that the reaction is essentially a nucleon-nucleon scattering, with the remaining ^3H as a spectator. The data available for $^3H\alpha \rightarrow n^6Li$ was σ from threshold to $E_t = 14$MeV obtained by detailed balance from measurments of $n^6Li \rightarrow t\alpha$ and $n^6Li^* \rightarrow t\alpha$ (G. Hale private communication). No data was available for $E_t > 18$MeV. For higher energies we used the cross-section for $^3He\alpha \rightarrow ^6Lip$

and $^3He\alpha \rightarrow {}^6Li^* p$ at $E_\alpha = 42$MeV and linearly interpolated between 14MeV and 42MeV. Unless there is some unexpected structure in the cross-section between these energies, the linear interpolation is accurate to within approximately 25%. The ^3H spectrum decreases exponetially with energy, so higher energies do not contribute to $\xi_{^6Li}$.

It is difficult to determine the magnitude of the errors introduced by these uncertainties; however, they could account for a 70% error in $\xi_{^6Li}/\xi_3$ and in $\xi_{^7Li}$.

The remaining uncertainties apply to all the ξ's; we list them in order of our estimate of their importance:

a)The inelasticity, ϵ, of inelastic baryon collisions is unknown in the energy range of interest (W. Bucza, private communication) and was taken to be between 0.4 and 0.75 , the extreme values communicated to us. The error in ϵ means that the number of scatterings of an energetic baryon before thermalization cannot be precisely determined. This leads to a large (approximately 50%) uncertainty in all the shower yields. We have checked that the uncertainty in the ratios of the yields ξ_i/ξ_j is smaller.

b) There is apparently no data on the energy distribution of the debris neutrons from inelastic $N-\alpha$ scattering. The debris neutrons contribute significantly to the shower yields. Their energies were taken to be $50-200$MeV. Low energy neutrons are effective ^3H producers, so uncertainty in their number manifests itself in an uncertainty in the ξ_d/ξ_3 ratio of approximately 20%.

c)Since neutrons are not thermalized by Coulomb scattering at 1GeV, they are more effective in destroying ^4He and synthesizing the other light elements than protons. An important source of neutrons is $pp \rightarrow pn\pi^+$. Since the neutron yield in nucleon-nucleon collisions is not well known below $E_N^{lab} \sim 3$GeV, the

number of energetic neutrons is uncertain.

d) The multiplicities and energies of jet baryons are not known at high energies. At 1TeV, the theoretical extrapolations are uncertain by a factor of two. As discussed in section 3.4 the effect of ν_B variation on the ξ's, has been explicitly included in the definition of r_B^*. Presumably, the effect of E_{in} variation on the ξ's can also be included in r_B^* through the factor $\mathcal{F}$. However we have not calculated the shower for $E_{in} > 10\text{GeV}$. It is possible that the ratio of ^7Li to the other light elements could be up to a factor of two smaller in high M_X scenarios.

e) There are large error bars in many of the experiments, especially those on $N - \alpha$ scattering (Meyer 1972). Different experiments at nearby energies often report different cross sections. The fits to the data are not always compelling.

f) The cross-over between strong interactions and Coulomb scattering as the dominant energy loss mechanism for protons is not a sharp boundary. It lies somewhere between 500MeV and 1GeV.

g) In the Compton thermalization of the photons, we ignored the logarithmic enhancement due to forward scattering, since it does not significantly alter the photon energy. A more careful treatment might slightly alter the effective strength of the Compton scattering term.

h) The energy distribution of the primary baryons was not considered. As discussed in (d), the dependence of the ξ's on the primary baryon energy can probably be embedded in r_B^*. However, this assumes that the primary baryons have a unique energy when actually they have some distribution of energies.

i) We ignored the destruction of light elements other than ^4He by very energetic ($E_n \gg 25\text{MeV}$, $E_p \geq 1\text{GeV}$) baryons. Since hadrodestruction of ^4He is a $O(10\%)$ effect, it will have approximately the same percentage effect on the

other light elements.

j) We have also neglected anti-nucleon destruction of the light elements. The cross-section for anti-nucleons to scatter off nucleons is $\sim 1/3$ the annihilation cross section. Hence, anti-nucleons do not multiple scatter and consequently do not produce significant baryonic showers. It is also possible for an anti-nucleon to destroy ^4He by annihilating a constituent nucleon. However, the total number of anti-nucleons produced is the same as primary nucleons, $r_B \nu_B f_X^o$. We shall see that this combination is $\lesssim 5 \ \ 10^{-3} f_p$. Therefore, the ^4He depletion, and hence other light element production, by anti-nucleons is negligible compared to the results of the baryonic showers.

k) In the treatments of Burns and Lovelace and Aharonian and Vardanian Delbruck ($\gamma\gamma \rightarrow \gamma\gamma$) scattering was ignored. It is possible to ignore Delbruck for $\Omega_B h_o^2 = 1$, because Compton scattering dominates. For $\Omega_B h_o^2 < 1$, the situation is less clear. This should be the subject of further investigation.

l) Our formula for Coulomb losses by energetic baryons is valid only for baryon velocities greater than the thermal velocity of the electrons in the plasma (D.Seckel, private communication). Since we are interested in abundances at freezeout, the relevant temperatures are $\sim 1keV$. A triton or helium-3 nucleus with a corresponding velocity would have a kinetic energy of only $\sim$ 6MeV. The threshold for ^6Li production is 8MeV triton energy with the bulk of production coming from tritons of $>$ 20MeV, so this should not be a major source of error in ξ_6. The threshold for $\alpha\alpha \rightarrow {}^7Lip$ is 36Mev in the lab frame and hence this has no effect on ξ_7.

m) As the X's decay, they add entropy to the system. In the parameter range of interest, this dilution is at the very most a factor of two and the time-

temperature relation is essentialy unaffected. However, for $\Omega_B h_o^2 \approx 1$, the corresponding initial η is higher, so there is a very slight increase in the initial abundance of ^4He coming from Standard Big Bang Nucleosynthesis. This will necessitate a small adjustment in equations 5.12 and 8.2.

For the sake of clarity, we will use the central values of the ξ's in all further discussions, unless otherwise specified. When needed, we will adopt the following estimates of the errors on the ξ's: 50% error in the overall normalization arising largely from the error in ϵ; 40% error in ξ_d/ξ_3 from the uncertainty in the debris neutron energy distribution, experimental error, and roundoff error in the shower calculation; 70% error in ξ_6/ξ_3 from the lack of data on $p\alpha \rightarrow {}^3H + \cdots$ and ${}^3H\alpha \rightarrow {}^6Lin$; 70% error in ξ_7, beyond the 50% in the overall normalization, from large (factor of 2) discrepancies in the data on $p\alpha$ elastic scattering at $E_{lab} \gtrsim$ 500MeV, and the sensitivity of the calculation to uncertainties in reading the data. We emphasize that our final abundances for the light elements, and hence the size of the allowed parameter space which we will derive for the X, depend crucially on the actual values of the ξ_i's.

5. Nuclear Abundances From Fixed Points

The equations for the light nuclear abundances (4.10)- (4.17) are too complicated to solve analytically. However, in each case a good approximation is to keep only the dominant production and destruction terms, where the equations take the form:

$$\dot{f} = J(t) - f\Gamma(t). \tag{5.1}$$

The behaviour of the solutions to (5.1) is discussed in detail in Appendix A, both for general J and Γ and for the three particular forms of which prove to be of interest. There we show that if

$$|\frac{\dot{J}}{J} - \frac{\dot{\Gamma}}{\Gamma}| \ll \Gamma, \tag{5.2}$$

then equation (5.1) reaches its fixed point $f(t) = J(t)/\Gamma(t)$, on time scales of order $t_r \approx \Gamma^{-1}$. Because the fixed point is time dependent we will refer to it as the state of quasi-static equilibrium (QSE). Equation (5.1) remains in QSE until either condition (5.2) is violated at a time t_c, or it freezes out at a time t_f. If $t_f < t_c$, then f freezes out at its QSE value.

The photon equation (4.18) is of the form (5.1), and has QSE solution:

$$f_{\gamma^*}(E) = \frac{\xi_{\gamma^*}(E) f_X^\circ \Gamma_X e^{-t/\tau_X}}{f_e n_{\gamma_{th}} c\sigma_C(E)} \tag{5.3}$$

The response time, t_r, is much less than τ_x at early times, so the photons rapidly approach QSE. Although $t_c < t_f$ for the photons (cf appendix), $t_c \gg \tau_x$. By the time the photon equation leaves QSE, J is exponentially small and $f_{\gamma^*} \approx 0$.

We now begin the arguments which identify the dominant destruction and production terms in (4.10) - (4.17). Except for the coupling between ^3He and the neutrons, these can easily be approximated by the form (5.1). The crucial point is that $n^3He \rightarrow {}^3Hp$ is important only at early times, before the onset of ^3He photo-dissociation, when both the proton density and the ratio of ^3He to protons is high. However, we are ultimately interested only in the final abundances. Since these are determined during the period of quasi- static equilibrium, when the temperature has already fallen to $\lesssim$ 10kev, and ^3He photodissociation has begun, we can ignore, for the purposes of these estimates, neutron depletion by ^3He. The simplified neutron equation,

$$\dot{f}_n = r_B^* \xi_n f_X^o \Gamma_X e^{-t/\tau_X} - f_n n_{\gamma_{th}} f_p (\sigma v)_{np \rightarrow d\gamma} - f_n \Gamma_n, \tag{5.4}$$

is decoupled, and is of the form (5.1). The QSE solution is therefore

$$f_n = \frac{r_B^* \xi_n f_X^o \Gamma_X e^{-t/\tau_X}}{n_{\gamma_{th}} f_p (\sigma v)_{np \rightarrow d\gamma} + \Gamma_n}. \tag{5.5}$$

We can now bring the remaining equations into the form (5.1). We add the ^3He and ^3H equations, and ^7Li and ^7Be equations, taking the photo-dissociation cross-sections of equal mass species to be equal, to obtain equations for the mass three and mass seven elements. Photodissociation of ^7Li and ^7Be is not an important source of ^6Li, because, in X decays, more ^6Li is produced than are ^7Li and ^7Be combined. We ignore the thermal neutron destruction terms for all these elements as they are small. The equations to which we apply the method of quasi-static equilibrium are therefore:

$$\dot{f}_d = r_B^* \xi_d f_X^o \Gamma_X e^{-t/\tau_X} + f_\alpha f_{\gamma^*} n_{\gamma_{th}} c\sigma_{\alpha\gamma\to d}\theta(E_{max} - Q_{\alpha\gamma\to d}) \quad (5.6)$$

$$+ f_p f_n n_{\gamma_{th}} (\sigma v)_{np\to d\gamma} - f_d f_{\gamma^*} n_{\gamma_{th}} c\sigma^D_{d\gamma}\theta(E_{max} - Q_d)$$

$$\dot{f}_3 = r_B^* \xi_3 f_X^o \Gamma_X e^{-t/\tau_X} + f_\alpha f_{\gamma^*} n_{\gamma_{th}} c\sigma_{\alpha\gamma\to 3}\theta(E_{max} - Q_{\alpha\gamma\to 3}) \quad (5.7)$$

$$- f_3 f_{\gamma^*} n_{\gamma_{th}} c\sigma^D_{3\gamma}\theta(E_{max} - Q_3)$$

$$\dot{f}_\alpha = -r_B^* \xi_\alpha^K f_X^o \Gamma_X e^{-t/\tau_X} - f_\alpha n_{\gamma_{th}} c f_{\gamma^*} \sigma^D_{\gamma\alpha}\theta(E_{max} - Q_4) \quad (5.8)$$

$$\dot{f}_{^6Li} = r_B^* \xi_{^6Li} f_X^o \Gamma_X e^{-t/\tau_X} \quad (5.9)$$

$$- f_{^6Li} n_{\gamma_{th}} (f_{\gamma^*} c\sigma^D_{\gamma^6 Li}\theta(E_{max} - Q_6) + f_n (\sigma v)_{n^6 Li\to t\alpha})$$

$$\dot{f}_7 = r_B^* \xi_7 f_X^o \Gamma_X e^{-t/\tau_X} - f_7 f_{\gamma^*} n_{\gamma_{th}} c\sigma^D_{7\gamma}\theta(E_{max} - Q_7), \quad (5.10)$$

where f_3,f_7,ξ_3,ξ_7, $\sigma^D_{3\gamma}$ and $\sigma^D_{\gamma 7}$ have their natural meanings, and the Q's are reaction threshold energies.

Can the equations (5.6)- (5.10) lead to acceptable abundances if $r_B = 0$? In appendix B we show that this is impossible: either too little ^4He is destroyed or too much ^3He is produced. This is why the program of Audouze et al (Audouze et al 1985) cannot succeed. Instead we rely on α destruction in hadronic showers to lower the ^4He abundance.

Dropping the photo-dissociation term from the α equation (which is consistent so long as $\tau_X \ll t_4$, the threshold for ^4He photo-dissociation), we integrate exactly to obtain :

$$f_\alpha(\infty) = f_\alpha(0) - r_B^* \xi_\alpha^K f_X^o. \quad (5.11)$$

Taking $\xi_\alpha^K = 10$, we find

$$r_B^*(f_X^o/f_b) = 1.15\ 10^{-3} - \frac{(Y - .24)}{40} \quad (5.12)$$

where Y is the final primordial-mass fraction of ^4He and f_p is the reduced number density of protons after primordial nucleosynthes. f_p is taken to be a constant since the net proton production is twice the number of ^4He's hadro-destroyed, hence $\Delta f_p/f_p \lesssim 4\%$.

Consider next equations for the other light element abundances. Several terms were discarded in this analysis. Since we do not permit the photo-dissociation of ^4He, we can drop this as a source term in all the equations. In the deuterium equation, the ratio of deuterium production in hadron showers to deuterium production from neutron capture by protons is

$$\frac{\xi_d}{\xi_n}(1+\frac{\Gamma_n}{n_{\gamma_{th}}(\sigma v)_{np\to d\gamma}f_p}) \gtrsim \frac{1}{6}(1+25(\frac{keV}{T})^3).$$

Thus although neutron capture by protons is comparable to shower production of deuterium, it is smaller at freezeout and can be ignored for the purpose of these estimates. Neutron capture can be disregarded as a sink for ^6Li. This is because the τ_X's that we will be forced to consider will be such that photo-dissociation will dominate neutron capture during the period of QSE, when the final ^6Li abundance is determined.

The equations for $\dot{f}_i$ $(i = D, ^3He, ^6Li, ^7Li)$ then take the form:

$$\dot{f}_i = (r_B^* \xi_i - c_i \frac{f_i}{f_p}) f_X^o \Gamma_X e^{-\Gamma_X t} \tag{5.13}$$

The c_i are defined by

$$c_i(t) = \frac{1}{\sigma_C} \int_0^{E_{max}(t)} \xi_{\gamma^*}(E)\sigma_{i\gamma}^D(E)dE \tag{5.14}$$

where we have ignored the energy and angular dependence of the Compton scattering. The times t_i are defined by $E_{max}(t_i) = Q_i$ the photodissociation threshold for nuclei i. For $t < t_i$ it is clear that $c_i(t)$ vanishes. Equation (5.13) has the form of (5.1), and since for $\tau_X > 2 \times 10^5 sec$, $t_c > t_i$, the abundances freeze-out with these fixed point values:

$$(\frac{f_i}{f_p})\Big|_{t=\infty} \approx \frac{r_B^* \xi_i}{c_i(t_f)}. \tag{5.15}$$

This is quite a remarkable result. The freeze-out values of c_i have only a weak dependence on i because the photodissociation cross-sections are all of order a millibarn. Hence, we predict that the ratios of these light element abundances are approximately just the ratio of the ξ_i

$$\begin{aligned} f_d : f_3 : f_{^6Li} : f_7 &\approx \xi_d : \xi_3 : \xi_{^6Li} : \xi_7 \\ &\approx 1 : 1 : 10^{-5} : 10^{-6}, \end{aligned} \tag{5.16}$$

compared with the values inferred from observation :

$$f_d : f_3 : f_{^6Li} : f_7 \approx 1 : 1 : (?) : 10^{-(5 to 6)}.$$

The success of these estimates is remarkable. The physics which determines these abundances is entirely different from the physics of the standard scenario; yet it yields approximately the same ratios of light element abundances. However, our scenario does make certain testable predictions. In particular, both the ^6Li to ^7Li and the ^3He to D ratios are higher than in the standard scenario. We will discuss this further in chapter 6, where we present our numerical results, and will show how it is reconciled with observations.

It is important to note that the ratios of these fixed point abundances are nearly independent of the properties of the X particle, and are therefore a non-trivial test of these ideas.

The light element abundances depend on the properties of X as follows:

1. The ^4He abundance depends only on $r_B^*(f_X^\circ/f_p)$,
2. The abundances of D, ^3He, ^6Li and ^7Li depend on the single parameter M_X/r_B^* as we now show. Taking $\sigma_{i\gamma}^D \simeq 1mb$ and $\sigma_C \simeq 30mb$, and using (4.2) in (5.14) gives

$$c_i \simeq \frac{M_X}{0.3GeV} \tag{5.17}$$

Using this in (5.15)gives

$$(\frac{f_i}{f_p})\Big|_{t=\infty} \approx r_B^* \xi_i (\frac{0.3GeV}{M_X}) \tag{5.18}$$

Successful abundances are thus obtained for

$$\frac{M_X}{r_B^*} \simeq 10^5 GeV \tag{5.19}$$

The numerical results of the next section confirm these results for a broad range of parameters.

We now consider the case $\Omega_B h_o^2 \neq 1$. The amount of requisite ^4He depletion is now different; equation (5.12)is replaced by

$$r_B^* \frac{f_X^\circ}{f_p} \simeq 1.5 \times 10^{-3} - 0.035(Y - 0.24) + 3.1 \times 10^{-4} \ln(\Omega_B h_o^2) \tag{5.20}$$

The abundances of the remaining light elements are still given by equation (5.15). r_B^* does not depend on $\Omega_B h_o^2$; ξ's have only a logarithmic dependence on $\Omega_B h_o^2$

arising from the electromagnetic Coulomb losses of equation (4.6); $c_i(t_f)$ of equation (5.14)has a mild sensitivity on $\Omega_B h_o^2$ from E_{max}. This arises from the dependence on the electron density of the crossover from pair creation to Compton scattering. Hence we obtain successful light element abundances for a wide range of $\Omega_B h_o^2$ including the previously excluded region of $0.03 \leq \Omega_B h_o^2 \leq 1.1$.

6.-Numerical Results

For the numerical analysis, we return to the full set of equations developed in section (2.3). Our program is as follows . We first solve the photon equation (4.18) analytically in the quasi-static limit, since the response time

$$\gamma^{-1} = (n_{\gamma_{th}} f_e c \sigma_C)^{-1} \approx 2(\frac{keV}{T})^3 sec \tag{6.1}$$

is much less than any other time scale in the problem. Using the solution to the photon equation, we solve the α equation (4.14) numerically. Throughout the program, we use the method of backward differencing because it provides greater numerical stability (Wagoner, private communication). We then solve the coupled neutron and ^3He equations ((4.19),(4.13)), then successively the ^3H equation (4.12) and the d equation (4.11), and the ^7Be equation (4.17), the ^7Li equation (4.16) and the ^6Li equation (4.15). In Fig. 5, we plot the abundances of the light elements as a function of t for representative values of M_X/r_B^*, τ_X, $r_B^*(f_X^o/f_p)$. A number of features are readily apparent:

a) At $t = 10^5 - 10^6$ seconds, the abundances of $d, ^3H, ^3He, ^6Li$, and ^7Li drop significantly. This represents the onset of photodestruction. The order in which the various elements begin to drop off is consistent with the ordering of the t_Q's as illustrated in figure 1.

b) Following the post-threshold drop, all the abundances, except that of ^7Be flatten out and do not change further. This is the onset of QSE. ^7Be of course continues to decay into ^7Li . This also explains the slight rise in the ^7Li abundance after the initial decline. One can also note the importance of ^3He and tritium photodissociation as a source of deuterium.

c) Except for ^4He the final abundances are independent of the initial abundances. All information about the initial conditions is quickly erased by shower production.

As expected, depletion of ^4He fixes $r_B^*(f_X^o/f_p)$ as per equation (5.12), $r_B^*(f_X^o/f_p) = 1.5 \times 10^{-3} - 0.033(Y_o - .24)$. This is valid for all M_X/r_B^* and M_X, and for $\tau_X \lesssim 6 \times 10^5$sec, when photodissociation of ^4He turns on. In Fig. 6, we plot the abundances of the light elements as a function of τ_x for representative values of M_X/r_B^*, and $r_B^*(f_X^o/f_p)$. We see that as τ_X is increased the various elements reach QSE before freeze-out. This is evidenced by the drop in the final abundances down to their QSE values. If τ_X is increased too far, ^4He becomes vulnerable to photodestruction while there is still some photon power. This causes the large rise in the ^3He abundance, and the much smaller rise in the D abundance. Li is of course unaffected.

Our next goal is to constrain M_X/r_B^* using the observed abundances of D,^3He,^6Li and ^7Li. We first note that our predicted ratio of ^6Li to ^7Li is $O(10)$, while observations indicate that presently $^6Li/^7Li \leq 1/10$ or possibly $1/20$. If we take the Pop II value of ^7Li as representing its primordial abundance, then, as in the standard scenario, we must assume that the lithium-7 in Pop I stars is non-primordial. Since the ^7Li abundance in Pop II is $O(10^{-10})$ we expect to produce $O(10^{-9})$ ^6Li. Although it is conceivable that ^6Li is depleted to the Pop I value of $\leq 10^{-10}$ within the Pop I star (as discussed for Pop II stars), the observed $^6Li/^7Li$ ratio of $< 1/10$ in the interstellar medium (Snell et al 1981) suggests that pre-Pop I stellar processing is necessary. To deplete the expected 10^{-9} to $\leq 10^{-10}$ requires approximately $50 - 90\%$ stellar processing. This results in a $50 - 90\%$ reduction in deuterium, and a smaller reduction or

even an increase[6] in ^3He and ^7Li. Such a scenario seems both plausible and likely to produce abundances consistent with observations. The exact amount of stellar processing required depends on the actual values of ξ_6 and ξ_7, which have large uncertainties, as well as on the values of M_X/r_B^* and τ_x.

If we take the Pop I ^7Li abundance of $\mathcal{O}(10^{-9})$ to be primordial, then we expect the primordial ^6Li abundance to be $\mathcal{O}(10^{-8})$. In order to reduce this ^6Li abundance to $\leq 10^{-10}$, we would require either that Pop I stars uniformly deplete their ^6Li or stellar processing of the pre-Pop I material with approximately $90-99\%$ efficiency. However, deuterium is destroyed to the same extent as ^6Li, while a sizable fraction of ^3He may remain. We expect the result to be a large helium-3 abundance and a small deuterium abundance. This is not a particularly attractive scenario and within our errors is excluded.

6

Let A be the fraction of primordial material which does not undergo stellar processing, and g_i be the fraction of element i which survives stellar processing in the "average" star, then $D_t = AD_p + (1-A)g_D D_p$ and $^3He_t \geq A\,^3He_p + (1-A)g_3(^3He_p + D_p)$ (Yang et al 1984). Here the subscript t indicates the pre-Pop I abundances and the subscript p denotes the primordial values. The D term in the ^3He equation comes from the conversion of deuterium to helium-3; ^3He can also be formed by incomplete H burning. g_D is generally taken to be zero, while g_3 is taken to be in the range $1/4 - 1/2$, although this number is model dependent and could be zero. ^6Li and ^7Li obey similar equations, although ^6Li is not a source of ^7Li; $g_6 \approx 0$, while g_7 could be of the order of g_3. ^7Li might also be produced in stars.

Returning to the scenario in which the Pop II ^7Li abundance is primordial, we constrain f_7 to lie in the interval $8 \times 10^{-11} - 2 \times 10^{-10}$. We then calculate the astration factors necessary to reduce the ^6Li abundance to $(0.25 - 1) \times 10^{-10}$. These are found to be anywhere from approximatel 15% to over 90%. We apply the astration factor to deuterium and helium-3, assuming $g_3 = 1/4$, and requiring for the astrated abundances $5 \times 10^{-6} < f_d < 5 \times 10^{-5}$ and $1 \times 10^{-5} < f_3 < 1.5 \times 10^{-4}$. We allow for 50% errors in the overall normalization of the ξ's, 40% errors in ξ_2/ξ_3, and 70% errors in ξ_6/ξ_3 and ξ_7/ξ_3 as discussed in the Uncertainties section of this paper. We find that M_X/r_B^* is constrained to be between $1 \times 10^4 GeV$ and $2 \times 10^5 GeV$, consistent with our predictions. τ_X is constrained to be between $2 \times 10^5 sec$ and $9 \times 10^5 sec$. In Fig. 7, we plot the allowed region in the M_X/r_B^* vs. τ_x plane for various amounts of astration. The upper limit on τ_X corresponds to the onset of ^3He production from ^4He photo-dissociation; the lower limit comes from the condition $t_c > t_Q$, so that freeze out happens after photo-dissociation of ^3He and ^3H has begun. In this region the astrated D and ^3He abundances vary over most of the allowed range,but consistently both the primordial and astrated $^3He/D$ ratio is greater than 1, as is the primordial ratio of ^6Li to ^7Li.

In Fig. 8, we plot our preferred range for M_X/r_B^* vs. τ_X, constraining deuterium to lie in the range $0.8 - 2 \times 10^{-5}$ and helium-3 in $1 - 6 \times 10^{-5}$. We find that we consistently require ξ_7 to be 70% higher than its calculated central value to obtain low ($< 75\%$) astration models. This is within the estimated errors for this quantity, but indicates that an improved value would be of interest.

In figure 9, we plot the primordial values of f_d, f_3, $f_{^6Li}$ and f_7 vs. M_X/r_B^* for several values of τ_X, using the central values of the ξ's. We see, once again ,

that consistently $f_3 > f_2$ and $f_6 \gtrsim f_7$, for the predicted primordial values.

As remarked in the previous chapter, it is important to note that $r_B^*(f_X^o/f_p)$ is determined exclusively by ^4He. M_X/r_B^* determines the overall scale of f_d, f_3, $f_{^6Li}$ and f_7 . M_X is entirely free (so long as $M_X \gtrsim 10\text{GeV}$). The approximate value of τ_x is a prediction.[7]

7

The analytic techniques applied in the previous chapter did well in predicting the light element abundances. If, as is likely, these techniques can be applied to other nucleosynthesis calculations, it should not be necessary to simply believe the output of complicated numerical programmes. By considering the dominant sink and source terms, one can gain a quantitative understanding of the results. We thank Bob Wagoner for suggesting this.

7. Testable Differences From the Standard Model

Our theory of nucleosynthesis predicts nuclear abundances that differ from those of the standard model. Although present observations cannot distinguish the two theories, improved future measurements of abundances should do so. The theories differ in their predictions of abundances in both primordial (unprocessed) matter and processed (eg. disk) matter. In table (Table 4), we contrast the predictions of the standard model with those of our theory for both primordal and disk matter. Note that the disk abundances depend on the amount of astration.

The most striking difference in primordial abundances occurs for ^6Li. We predict a ^6Li abundance which is more than thirty times bigger than that of the standard model. We also predict higher $D, ^3He$, and $^3He/D$ and slightly lower ^7Li. A subset of these differences could potentially be tested by looking at quasar spectral lines.

As far as disk matter, we predict more $^6Li, ^3He$, and $^3He/D$ than the standard model.

Finally, our theory can accomocdate an ^7Li abundance that is smaller than that of the standard model, as well as *any* ^4He abundance which is less than or equal to that of the standard big bang. Any observation that suggests that the ^4He or ^7Li abundances are lower than previously thought would be evidence against the standard model, but would be consistent with our theory.

8. Discussion of Results and Conclusions

In this paper we have analyzed the synthesis and destruction of light elements in the keV era of the hot big bang via hadronic and electromagnetic showers induced by the decays of heavy particles. We have found primordial abundances of d, ^3He, ^4He ^6Li and ^7Li for $\Omega_B h_o^2$ equal to or less than unity, which, within our uncertainties, are in agreement with observations.

We have shown that cosmologies with $0.03 < \Omega_B \leq 1.1$ are consistent with primordial nucleosynthesis if there is a particle X with properties:

$$2 \times 10^5 sec < \tau_X < 9 \times 10^5 sec \tag{8.1}$$

$$r_B^* \frac{f_X^o}{f_B} = 1.15 \times 10^{-3} - (\frac{Y - 0.24}{40}) + 2.2 \times 10^{-4} \ln h_o^2 \Omega_B \tag{8.2}$$

$$\frac{1}{200} < r_B^* \frac{1000 GeV}{M_X} < \frac{1}{10} \tag{8.3}$$

We have commented on how these parameters might arise in section II. If τ_X is outside the range of (8.1) the scheme does not work. Equation (8.2) is the condition for obtaining an acceptable ^4He mass fraction Y, and (8.3) is required to obtain acceptable primordial d, ^3He, ^6Li and ^7Li abundances.

We have described a scheme in which nucleosynthesis occurs in two stages. A conventional era at $T \sim 30 - 100$ keV and a new era at $T \sim$keV. In fact our results do not depend on wether there ever was such a conventional era. We require only that above a few keV, the ^4He abundance is larger than its observed primordial value. The initial conditions for d, ^3He, and ^7Li are completely irrelevant, since no memory of them survives once the evolution equations reach

their fixed point. Therefore the only memory of physics at temperatures above a keV is the existence of a substantial ^4He abundance.

The standard $\Omega = 1$ cosmology of the hot big bang has conventional nucleosynthesis with $0.014 < \Omega_B h_o^2 < 0.03$. The dark matter includes exotic particles which are stable and which have masses and couplings chosen so that the exotic contribution to Ω is 10-100 times the baryonic contribution.

We have proposed an alternative scheme for accommodating $\Omega = 1 : \Omega_B = 1$, with a keV era of unconventional synthesis and destruction of the light elements. This requires an exotic unstable particle with parameters chosen to give the correct ^4He and d abundances.

This alternative scheme provides motivation for exploring the possibility of a completely consistent cosmology with $\Omega_B = 1$. This would require understanding the formation of large scale structure in such universes with $\Omega_B = 1$ (Peebles 1987a,b) the present form and location of the dark matter, and how we could observe this dark matter to be baryonic.

In addition our scheme for nucleosynthesis can accommodate any $\Omega_B h_o^2$ between 0.014 and 1.1 . Hence study of the formation of large scale structure and dark matter in these universes is also of interest (Peebles 1987a,b and Blumenthal et al 1987)

The model does have definite, hopefully testable, predictions, which distinguish it from standard Big Bang nucleosynthesis.

We predict that the primordial $^3He/D$ ratio is greater than one and that the primordial abundance of ^6Li is of the same order as or larger than that of ^7Li. We predict that in the disk $^3He, ^6Li$ and $^3He/D$ are higher than in the standard model. Finally, it seems possible, in light of recent observations, that

the primordial ^4He abundance is lower than had been previously believed. If this proves to be so, then standard Big Bang nucleosynthesis may not be able to explain both the observed deuterium and helium-4. Since the ^4He abundance in our model is essentially independent of the abundances of the other light elements, we would regard it merely as a revised prediction for $r_B^*(f_X^o/f_p)$ as a function of $\Omega_B h_o^2$.

APPENDIX A

Fixed point analysis for source-sink equations

In this appendix we derive the analytic solution to the equation

$$\dot{f} = J(t) - f\Gamma(t) \qquad J, \Gamma \geq 0. \tag{A.1}$$

The general solution to equation (A.1) is

$$f(t) = e^{-\int_{t_i}^{t} \Gamma(t')dt'} \left[f(t_i) + \int_{t_i}^{t} J(t') e^{+\int_{t_i}^{t'} \Gamma(t'')dt''} dt' \right], \tag{A.2}$$

where t_i is the initial time, which we take to be $t = 0$. If J and Γ are constants this can be integrated exactly to obtain

$$f(t) = e^{-\Gamma t}\left(f_o - \frac{J}{\Gamma}\right) + \frac{J}{\Gamma}. \tag{A.3}$$

On time scales of order Γ^{-1}, this approaches the equilibrium value J/Γ. Now in general J and Γ are time dependent. Making the ansatz

$$f = \frac{J}{\Gamma} + \delta, \tag{A.4}$$

we find that

$$\dot{\delta} = -\Gamma\delta - \frac{J}{\Gamma}\left[\frac{\dot{J}}{J} - \frac{\dot{\Gamma}}{\Gamma}\right]. \tag{A.5}$$

If

$$\left|\frac{\dot{J}}{J} - \frac{\dot{\Gamma}}{\Gamma}\right| \ll \Gamma, \tag{A.6}$$

then δ becomes much less than J/Γ in a response time, t_r, such that

$$\int_t^{t+t_r} \Gamma(t')dt' \sim 1. \tag{A.7}$$

Therefore, so long as condition (A.6) holds, f approaches its fixed point value, $f = J/\Gamma$, which we previously referred to as the state of quasi-static equilibrium (QSE). If condition (A.6) is violated at a time t_c, then f leaves quasi-static equilibrium.

If, at some time t, $\int_t^\infty J dt' \ll f(t)$, then f does not grow appreciably after t; if also $\int_{t_c}^\infty \Gamma dt \ll 1$, then f does not diminish appreciably. We define t_f as the time when both these conditions are met; we say that f freezes out,

$$f(t = \infty) \approx f(t_f).$$

If $t_f < t_c$ then f freezes out at its QSE value

$$f(t = \infty) \approx \frac{J(t_f)}{\Gamma(t_f)}.$$

There are three particular cases which are of interest to us:

Case I: $J = \jmath e^{-t/\tau}$; $\jmath, \Gamma$ constant

This is the form of the neutron equation ((5.4)) when only the decay term is included as a sink (this is valid well before t_f) . In this case, the solution (A.2) can be expressed in terms of known functions.

$$f(t) = \frac{\jmath e^{-t/\tau}}{\Gamma - \frac{1}{\tau}}(1 - e^{-\Gamma t}) + e^{-\Gamma t} f(0). \tag{A.8}$$

If $\Gamma^{-1} \ll \tau$, then, for $t \gg \Gamma^{-1}$,

$$f(t) \approx \frac{\jmath e^{-t/\tau}}{\Gamma}. \tag{A.9}$$

Case II: $J = \jmath(t)e^{-t/\tau}$, $\Gamma(t) = \varsigma t^{-n}$; $\jmath, \varsigma$ constant, $n > 0$

The photon equation ((4.18)) is of this form. In this case, condition (A.6) becomes

$$\left|\tfrac{1}{\tau} + \tfrac{n}{t}\right| \ll \Gamma. \tag{A.10}$$

This is satisfied if $t \ll (\varsigma\tau)^{1/n}$ and $t \ll (\varsigma/n)^{\frac{1}{n-1}}$. Thus

$$t_c \approx min((\varsigma\tau)^{1/n}, (\frac{\varsigma}{n})^{\frac{1}{n-1}}) \tag{A.11}$$

and

$$t_f = (\frac{n-1}{\varsigma})^{\frac{1}{1-n}}. \tag{A.12}$$

Case III: $J = \jmath(t)e^{-t/\tau}$, $\Gamma(t) = \gamma(t)e^{-t/\tau}$; $\jmath$ constant

The equations for d ((5.6)), ${}^3H + {}^3He$ ((5.7)), ${}^6Li$ ((5.9)), and ${}^7Li + {}^7Be$ ((5.10)) are brought into this form.

If γ is a constant, then the solution (A.2) can again be integrated exactly to obtain

$$f(t) = e^{\gamma\tau(e^{-t/\tau}-1)}f_o + \frac{\jmath}{\gamma}(1 - e^{\gamma\tau(e^{-t/\tau}-1)}) \tag{A.13}$$
$$\xrightarrow{t\to\infty} \quad \frac{\jmath}{\gamma} + e^{-\gamma\tau}(f_o - \frac{\jmath}{\gamma}).$$

If $\gamma\tau \gg 1$, then the correction to $\jmath/\gamma$ is small.

If γ is time dependent, the QSE solution is

$$f(t) = \frac{\jmath(t)}{\gamma(t)}. \tag{A.14}$$

Condition (A.6) becomes

$$|\frac{\dot{\gamma}}{\gamma}| \ll \gamma e^{-t/\tau}. \tag{A.15}$$

For any particular form of γ, one can compute t_f and t_c and check whether $t_f < t_c$. In the equations of interest, γ is of the form

$$\gamma(t) = \begin{cases} \gamma_o(1 - (\frac{t}{t_s})^{-n}) & t > t_s \\ 0 & \text{otherwise}, \end{cases} \tag{A.16}$$

with $0 < n < 1$. Then $t_f \leq \tau ln\gamma_o\tau$ and t_c is the larger of the two roots of

$$1 = \frac{\gamma_o}{n}(\frac{t}{t_s})^{n+1}(1 - (\frac{t}{t_s})^{-n})^2 \;\; e^{-t/\tau}. \tag{A.17}$$

If the smaller root, t_{on} , is greater than t_s then it represents a critical time for the onset of QSE. Note that there is also a critical $\gamma_o = \gamma_c$ such that (A.17)has any roots. In all the equations of interest $\gamma_o > \gamma_c$ and $t_{on}, t_s < t_f < t_c$. The final abundances are therefore approximately the QSE abundances at freeze-out.

APPENDIX B

The Necessity for Baryonic Decays of X

As Ω_B is increased to unity, the conventional era of nucleosynthesis produces progressively more ^4He and ^7Li and less d and ^3He. In this appendix we show that a condition for X decays to give acceptable adjustments to these abundances is that r_B must be non-zero. That is, we show that electromagnetic showers induced by photons, leptons or mesons cannot photodestroy ^4He and ^7Li and synthesize D and ^3He by the desired amounts.

At first sight a scheme with only electromagnetic showers from X decays appears promising. A large ^7Li photodestruction and a much smaller ^4He photodestruction can be arranged by choosing $\tau_X \sim t_7$, since in this case only a fraction e^{-t_4/τ_X} of X's decay after t_4 when ^4He is vulnerable. The photodissociation of ^4He will lead to n, D and other remnants. Some of the neutrons will be captured by protons to form D before they decay. Hence this scenario also has a mechanism for deuterium production. The majority of the deuterium which is made will be photodissociated. However, the tail of the ^4He destruction will lead to D which have large survival probabilities, since they are made late enough that few X's remain to decay.

This simple and appealing picture for the adjustment of the ^7Li, ^4He and D abundances by electromagnetic showers is ruined by the overproduction of ^3He. This can be seen by just considering the coupled ^3He and ^4He equations. Suppose that most of the ^4He is destroyed after $\tilde{t}_4$, where $\tilde{t}_4$ is the time at which

$\sigma^D_{\gamma_4}$ has reached a sizable fraction of its maximum value. Then for $t > \tilde{t}_4$

$$\dot{f}_4 = -c_4 f_4 f^o_X \Gamma_X e^{-\Gamma_X t} \tag{B.1}$$

$$\dot{f}_3 = (c_4 f_4 - c_3 f_3) f^o_X \Gamma_X e^{-\Gamma_X t} \tag{B.2}$$

Here f_3 can be taken to be the sum of the scaled ^3H and ^3He number densities, and c_3 will involve an appropriate average of the photodestruction ratios of ^3H and ^3He. For times late enough that ^4He can be photodestroyed to D, the c_4 in (B.2)is slightly smaller than the c_4 in (B.1). This small correction will not affect our argument.

Since $t > \tilde{t}_4$ and since f_4 is only to be reduced by $\mathcal{O}(10\%)$, it is a good approximation to take c_3, c_4 and f_4 as constants in the right hand sides of these equations. It is then straightforward to integrate (B.2)and use the fact that $c_4 f_4 \gg c_3 f_3(\tilde{t}_4)$ to obtain

$$\frac{f_3(\infty)}{f_4(\infty)} = \frac{c_4}{c_3}(1 - exp(-c_3 e^{-\Gamma_X \tilde{t}_4})) \tag{B.3}$$

This ratio of abundances is never small. If $c_3 e^{-\Gamma_X \tilde{t}_4} > 1$, the condition for f_3 reaching quasi-static equilibrium is satisfied so that $\frac{f_3}{f_4} \simeq \frac{c_4}{c_3}$, the fixed point of (B.2). If $c_3 e^{-\Gamma_X \tilde{t}_4} < 1$, the exponential can be expanded so that $\frac{f_3}{f_4} \simeq c_4 e^{-\Gamma_X \tilde{t}_4}$. From the solution to (B.1), this quantity is seen to be the fractional destruction of ^4He, which must be taken to be $\mathcal{O}(\frac{1}{10})$. This case corresponds to a ^3H or ^3He being produced for each ^4He destroyed; photodissociation of ^3H or ^3He being unimportant. We conclude that if ^4He destruction occurs predominantly after $\tilde{t}_4$, then either too little ^4He is destroyed or too much ^3He is produced.

This leaves open the possibility that sufficient ^4He is destroyed between t_4 and $\tilde{t}_4$. If the destruction occurs sufficiently close to t_4, then $c_4 \ll c_3$. The most optimistic case for a small f_3/f_4 ratio would be for (B.2)to reach QSE and then freeze out rapidly so that

$$\frac{f_3}{f_4} \simeq \frac{c_4(t_4+\delta)}{c_3},$$

where freezout occurred at $t = t_4 + \delta$ and $\delta \ll t_4$. Since $\sigma^D_{\gamma_4}$ is approximately proportional to δ for small δ, $f_3/f_4 \lesssim 10^{-3}$ requires $\delta/t_4 \lesssim 10^{-3}$. For significant ^4He destruction during the time interval δ after t_4, significantly more X decays must occur at, say, $t_4 + \delta/2$ than at $t_4 + \delta$. This requires $\tau_X < \delta \lesssim 5 \times 10^3$ seconds. However, if τ_X were this small, the fraction of X's remaining by t_4 is $e^{-t_4/\tau_X} \lesssim e^{-1000}$. This case is therefore not only fine tuned, but also leads to the requirement of an absurdly large value for f^o_X. Of course, ^7Li would be over-depleted by a very large factor.

We have shown that a scenario with $\Omega_B = 1$ and X having only non-baryonic decays does not work: too large a value for the primordial $^3He/^4He$ abundance is produced. Thus $M_X < m_{proton}$ is completely excluded. Any successful $\Omega_B = 1$ scenario which utilizes late decays must consider the complications of baryonic showers. Furthermore, this analysis suggests that it is better to reduce the ^4He abundance by baryodestruction rather than by photodissociation.

Acknowledgements

It is a pleasure to thank Ann Boesgaard, David Schramm, Mike Turner and especially Bob Wagoner for very valuable discussions and suggestions. We would also like to thank Bob Wagoner for the use of the output from his code.

S.D. and G.D.S. acknowledge support by the National Science Foundation under Grant NSF-PHY-86-12280 to Stanford University. G.D.S. is a National Science and Engineering Research Council of Canada Postgraduate Scholar. R.E. acknowledges support by the Department of Energy, contract DE-AC03-76SF00515 at SLAC. L.J.H. acknowledges support by the Director, Office of Energy Resources, Office of High Energy and Nuclear Physics, Division of High Energy of the U. S. Dept. of Energy under contract DE-AC03-7600098 and in part by NSF under Grant PHY-85-15857. L.J.H. also acknowledges partial support by a Sloan Foundation Fellowship and a Presidential Young Investigator Award.

REFERENCES

Aharonian,F.A. and Vardanian,V.V. 1985,

Yerevan Physics Institute preprint 827(54)-85 .

Alcock,C.A., Fuller,G.M., and Mathews,G.J. 1987, **LLL** preprint.

Andersen,J., Gustaffson,B. and Lambert,D.L. 1984 *Astr. Ap.*, **136** , 65.

Applegate,J.H., Hogan,C.J. and Scherrer,R.J. 1987, *Phys.Rev.*, **35D**, 1151.

Audouze,J. et al 1983, *Astr.Ap.*, **127**, 164.

Audouze,J., Lindley,D., and Silk,J. 1985, *Ap.J.* , **293** , L53.

Bania, T.M., Rood, R.T., and Wilson, T.L. 1987, preprint.

Berman,B.L. 1975, *Atomic Data and Nuclear Tables*, **15**, 339.

Blumenthal,G.R., Dekel,B.A. and Primack,J.R. 1987, preprint **SCIPP** 87/81.

Blumenthal,G.R., Faber,S.M., Flores,R. and Primack,J.R. 1986, *Ap.J.*, **301**, 27.

Boesgaard,A.M. and Steigman,G. 1985, *Ann.Rev.Astr.Ap.*, **23**, 319.

Bresser,G., Bass,R. and Kruger,K. 1969, *Nucl. Phys.* , **131A** , 679-697.

Brown,R.E. and Koepke,J.A. 1977, *Phys. Rev.* , **16C** , 18.

Brown,R.E., Ohlsen,G.G., Haglund,R.F.,Jr. and Jarmic,N. 1977, *Phys. Rev.*, **16C**, 513.

Burns,M.L. and Lovelace,R.V.E. 1982, *Ap. J.*, **262**, 87.

Cayrel,R.,Cayrel de Strobel,G.,Campbell,G.,Dappen,W. 1984, *Ap.J.*, **283**, 205.

Dimopoulos,S.,Esmailzadeh,R.,Hall,L.J., Starkman,G.D. 1987,

"Gravitino Cosmologies with Large Ω_B," preprint **SLAC-PUB-4357**.

Dominguez-Tenreiro,R. 1987, *Ap.J.*, **313**, 523.

Dupree, A.K., Baliunas, S.L., and Shipman, H.L. 1977, *Ap. J.*, **218**, 361.

Encrenaz, T., and Combes, M. 1982., *Icarus*, **52**, 54.

Faul,D.D., Berman,B.L., Meyer,P. and Olson,D.L. 1981, *Phys. Rev.*, **24C**, 849.

Fowler,W.A., Caughlan,G.R. and Zimmerman,B.A. 1967, *Ann.Rev.Astr.Ap.*, **5**, 525.

Glagola,B.C., Mathews,G.J., Breuer,H.F., Viola,V.E.,Jr., Roos,P.G., Nadasen,A. and Austinj,S.M. 1978, *Phys.Rev.Lett.*, **41**, 1698.

Gorbunov,A.N. and Spiridonov,V.M. 1958, *Soviet Physics JETP*, **34(7)**, 596.

Gorbunov,A.N. and Spiridonov,V.M. 1958, *Soviet Physics JETP*, **34(7)**, 600.

Gorbunov,A.N. and Varfolomeev,A.T. 1964, *Phys.Lett.*, **11**, 137.

Govarets,J., Lucio,J.L., Martinez,A. and Pestiau,J. 1981, *Phys.Rev.*, **24C**, 849.

Gry, C., Laurent, C., Vidal-Madjar, A. 1983, *Astron. Astrophys.*, **124**, 99.

Gry, C., Lamers, H.J.G.L.M., Vidal-Madjar, A. 1984, *Astron. Astrophys.*, **137**, 29.

Halbert,M.L., van der Woude,A. and O'Fallon,N.M. 1973, *Phys.Rev.*, **8C**, 1621.

Hubbard, W.B., and MacFarlane, J.J. 1980, *Icarus*, **44**, 676.

Jackson,J.D. 1974 , in *Phenomenology of Particles at High Energies*, ed. R.L.Crawford and R.Jennings, New York Academic Press.

Jackson,J.D. 1975, *Classical Electrodynamics* Wiley, N.Y.

King,C.H., Rossner,H.H., Austin,S.M., Chien,W.S., Mathews,G.J., Viola,V.E.,Jr. and Clark,R.G. 1975 *Phys.Rev.Lett.*, **35**, 988.

Klem,R. et al 1977, *Phys.Lett.*, **70B**, 155.

Koepke,J.A. and Brown,R.E. 1977, *Phys.Rev.*, **16C**, 18.

Kozlovsky,B. and Ramaty,R. 1974, *Astr.Ap.*, **34**, 744.

Kunth, D. 1983, in *ESO Workshop on Primordial Helium*, Garching, 335.

Lindsay,R.H., Toews,W. and Veit,J.J. 1973, *Nucl.Phys.*, **199A**, 513.

Maurice,E., Spite,F. and Spite,M. 1984, *Astr.Ap.*, **132**, 278.

Meneguzzi,M., Audouze,J. and Reeves,H. 1971, *Astr.Ap.*, **15**, 337.

Merchez,F., Bovchez,R. and Yarin,A.I. 1972, *Nucl.Phys.*, **182A**, 428.

Meyer,J.P. 1972, *Astr.Ap.Suppl.*, **7** 417, a.k.a. "The Bible ".

Miljanic,D., Furic,M. and Valkovic,V. 1970, *Nucl.Phys.*, **148A**, 312.

Mitler,H.E. 1972, *Astr.Sp.Sc.*, **17**, 186.

Neutron Standard Reference Data (1972) (99) 144

Nuclear Cross Sections and Technology, Vol. 1,p.244

Pagel,B.E.J. 1982, *Phil.Trans.R.Soc.A.*, **307**, 19.

Peebles,P.J.E. 1966, *Ap.J.*, **146**, 542.

Peebles,P.J.E. 1987a, " Yet Another Scenario for Galaxy Formation "
Princeton University preprint.

Peebles,P.J.E. 1987b, "Origin of the Large Scale Galaxy Peculiar Velocity Field:
A Minimal Isocurvature Model," Princeton University preprint.

Primack,J.R. 1984, preprint SLAC-PUB-3387, Lectures given at International
School of Physics, Enrico Fermi, Varenna, Italy, June 26 - July 6, 1984.

Proceedings of the international conference on the interactions of neutrons with nuclei,Lowell 1976

Rebolo,R. et al 1986, *Astr.Ap.*, **166**, 195.

Reeves,H. 1974, *Ann.Rev.Astr.Ap.*, **12**, 437.

Rood, R.T., Bania, T.M., and Wilson, T.L. 1984, *Ap. J.*, **280**, 629.

Rossorio-Garcia,E. and Beason,R.E. 1977 *Nucl.Phys.*, **275A**, 453.

Schwitters,R.F. 1983, *Proceedings of the 11th SLAC Summer Institute on Particle Physics , Stanford CA, July 18-29, 1983,* SLAC-0267 .

Snell, R.L., Vanden Bout, P.A. 1981, *Ap. J.*, **250**, 160.

Sowerby,M.G., Patrick,B.H., Utley,C.A. and Diment,K.M. 1970, *J.Nucl.Energy*, **24**, 323.

Spiger,R.J. and Tombrello,T.A. 1967, *Phys.Rev.*, **163**, 964.

Spite,F., Maillard,J.P. and Spite,M. 1984, *Astr.Ap.*, **141**, 56.

Spite,F. and Spite,M. 1982, *Astr.Ap.*, **115**, 357.

Stephany,W.P. and Knoll,G.F. , *Bull.Am.Phys.Soc.,Series II*, **20**, 144.

Steigman, G., Gallagher, J.S.III, and Schramm, D.N. 1987, preprint PRINT-87-0267 (Ohio State).

Trauger,J.T., Roesler,F.L., Carleton,N.P. and Traub,W.A. 1973, *Ap.J.Lett.*, **184**, L137.

Valkovic,V., Paic,G., Salus,I., Tomas,P. Cerino,M. and Satchler,G.R. 1965, *Phys.Rev.*, **139B**, 331.

Vidal-Madjar, A., Laurent, C., Gry, C., Bruston, P., Ferlet, R., and York, D.G. 1983, *Astron. Astrophys.*, **120**, 58.

Wagoner,R.V. 1967, *Science*, **155**, 1369.

Wagoner,R.V. 1968, *Ap.J.Suppl.*, **18**, 247.

Wagoner,R.V., Fowler,W.A. and Hoyle,F. 1967, *Ap.J.*, **148**, 493.

Wong,C.F., Hutcheon,R.M., Shin,Y.M. and Caplan,H.S. 1970, *Can.J.Phys.*, **48**, 1917.

Yang,J., Turner,M.S., Steigman,G., Schramm,D.N. and Olive,K.A. 1984, *Ap.J.*, **281**, 493.

FIGURE CAPTIONS

1) E_{max} as a function of time. The times when the various elements become susceptible to photodestruction are indicated.

2) The post pair production "breakout" spectrum of energetic photons at 10^6s, arising from the decay of an X with $M_X = 100$GeV.

3) The contribution of one 5GeV n to a baryon shower. On each branch, the probability of taking that branch from the parent node is indicated. The final yields of suprathermal $^4He, ^3He, ^3H, d$, and n's, and the number of background α's destroyed, are indicated below

4) The reactions which determine the abundances of the light elements

5) Abundances of the light elements as a function of time for $M_X/r_B^* = 7 \times 10^4$GeV , $r_B^*(f_X^o/f_p) = 1.27 \times 10^{-3}$, $\tau_x = 4.5 \times 10^5$s , with ξ_7 equal to 1.7 times its central value and $\xi_{^6Li} = \xi^c_{^6Li}$.

6) Abundances of the light elements as a function of X lifetime for $M_X/r_B^* = 7 \times 10^4$GeV , $r_B^*(f_X^o/f_p) = 1.27 \times 10^{-3}$. ^3H eventually decays into ^3He and so is included in the final ^3He abundance.

7) The allowed region in the $M_X/r_B^* - \tau_X$ plane for 30%,40%,50%, 60%,75% and 90% astration.

8) Preferred range of M_X/r_B^* and τ_X

9) Abundances of the light elements as a function of M_X/r_B^* for $r_B^*(f_X^o/f_p) = 1.27\ 10^{-3}$, and $\tau_X = 3, 4, 5\ 10^5$s. a)D, b) ^3He and c) ^6Li and ^7Li.

Table 1. Reactions contributing to baryon shower development

1_p	$pp \rightarrow pp$
2_p	$pp \rightarrow pp\pi's$
3_p	$pp \rightarrow pn\pi's$
4_p	$np \rightarrow np$
5_p	$np \rightarrow np\pi's$
6_α	$p^4He \rightarrow p^4He$
7_α	$p^4He \rightarrow p^4He\pi's$
8_α	$p^4He \rightarrow n^4He\pi's$
9_α	$p^4He \rightarrow np^3He$
10_α	$p^4He \rightarrow 2p^3H$
11_α	$p^4He \rightarrow p2d$
12_α	$p^4He \rightarrow 2pnd$
13_α	$p^4He \rightarrow 2n3p$
14_α	$n^4He \rightarrow n^4He$
15_α	$n^4He \rightarrow n^4He\pi's$
16_α	$n^4He \rightarrow np^3H$
17_α	$n^4He \rightarrow 2n^3He$
18_α	$n^4He \rightarrow n2d$
19_α	$n^4He \rightarrow p2nd$
20_α	$n^4He \rightarrow 3n2p$

Table 2. Hadron shower yields

Yields	$\epsilon = 0.25$	$\epsilon = 0.60$
ξ_{α}^{K}	-15	-7
ξ_{d}	7	3
$\xi_{^3H}$	6	2.5
$\xi_{^3He}$	4	1.5
$\xi_{^4He^*}$	7	3.5
$\xi_{^6Li}$	7×10^{-5}	3×10^{-5}
$\xi_{^7Li}$	2.5×10^{-6}	1×10^{-6}
$\xi_{^7Be}$	2.5×10^{-6}	1×10^{-6}
ξ_{n}	18	9

Table 3. A compilation of all the data used

Reaction	Energy Range	Useful Data	Reference
$^4He(\alpha,p)^7Li$	$30-120$ MeV	σ_{total}	Mitler 1972
$^4He(\alpha,p)^7Li,^7Li^*$	$30-110$ MeV	σ_{total}	Kozlovsky and Ramaty 1974
$^4He(\alpha,p)^7Li$	$60-140$ MeV	σ_{total}	King et al 1975
$^4He(\alpha,p)^7Li$	$40-180$ MeV	σ_{total}	Glagola et al 1978
$^4He(\alpha,p)^7Li$	$40-400$ MeV	σ_{total}	Meneguzzi et al 1971
$^4He(\alpha,n)^7Be$	$40-180$ MeV	σ_{total}	Glagola et al 1978
$^4He(^3He,p)^6Li$	$10,28,40$ MeV	$\frac{d\sigma}{d\Omega_{cm}},\sigma_{total}$	Koepke and Brown 1977
$^4He(\alpha,x)^6Li$	$40-180$ MeV	σ_{total}	Glagola et al 1978
$^4He(\alpha,x)^6Li$	$60-$ MeV	$\sigma_{total},\sigma^x_{partial}$	Mitler 1972
$^4He(\alpha,x)^6Li$	$40-1000$ MeV	σ_{total}	Meneguzzi et al 1971
$^3H(\alpha,n)^6Li$	$0-14$ MeV	σ_{total}	G.Hale, private communication
$^6Li(n,x)$	$4-7$ MeV	$\sigma^x_{partial}$	Rossorio-Garcia and Beason 1977
$^6Li(n,p)^6He$	$3-9$ MeV	σ_{total}	Bresser et al 1969
$^6Li(n,\alpha)t$	$10-150$ keV	σ_{total}	Sowerby et al 1970
$^6Li(n,\alpha)^3H$	964 keV	σ_{total}	Stephany and Knoll
$^6Li(n,t)^4He$	$100-600$ MeV	$\frac{d\sigma}{d\Omega}(0^\circ)$	Brown et al 1977
$^6Li(n,\alpha)t$	100eV-20 MeV	σ_{total}	Nuclear Cross Sections
$^6Li(n,t)^4He$	27 MeV	$\frac{d\sigma}{d\theta_{cm}}$	Proceedings, Lowell 1976
$^6Li(n,\alpha)^3H$	$10-1000$ keV	σ_{total}	Neutron Standard Ref. Data 1972
$^6Li(n,x)$	200eV-2 MeV	$\sigma_{absorption}$	Sowerby et al 1970
$^6Li(n,d)^5He$	14.4 MeV	$\frac{d\sigma}{d\theta_{cm}}$	Valkovic et al 1965
$^6Li(n,\gamma)^7Li$	10eV-10 MeV	σ_{total}	Nuclear Cross Sections
$^6Li(n,p)^6He$	$3-10$ MeV	σ_{total}	Proceedings, Lowell 1976

Reaction	Energy Range	Useful Data	Reference
$^6Li(n,n'd)^4He$	$0-20$ MeV	σ_{total}	Proceedings, Lowell 1976
$^6Li(n,2np)^4He$	$0-20$ MeV	σ_{total}	Proceedings, Lowell 1976
$^6Li(n,p)^6He$	14 MeV	$\frac{d\sigma}{d\theta_{cm}}$	Merchez et al 1972
$^6Li(n,\gamma)^7Li$	$\lesssim 1$ MeV	$(\sigma v)_{capture}$	Fowler et al 1967
$^6Li(p,\ )$	$10^{-2}-10^4$ MeV	$\sigma^{destruction}$	Reeves 1974
$^7Li(n,\ )$	14.8 MeV	$\frac{d\sigma}{d\Omega_{cm}}$	Lindsay et al 1973
$^7Li(n,t)^5He$	14.4 MeV	$\frac{d\sigma}{d\Omega_{cm}}$	Proceedings, Lowell 1976
$^7Li(n,t),(n,d)$	$3-15$ MeV	$\frac{d\sigma}{d\Omega_{cm}dE}$	Miljanic et al 1970
$^7Li(n,\gamma)^8Li$	$\lesssim 1$ MeV	$(\sigma v)_{capture}$	Fowler et al 1967
$^7Li(p,\ )$	$10^{-2}-10^4$ MeV	$\sigma^{destruction}$	Reeves 1974
$^7Be(n,p)^7Li$	$\lesssim 1$ MeV	$(\sigma v)_{capture}$	Fowler et al 1967
$^3He(n,p)^3H$	$0.1-10$ MeV	$\sigma_{total}, \frac{d\sigma}{d\Omega}$	Nuclear Cross Sections
$^3He(n,p)^3H$	$\lesssim 1$ MeV	$(\sigma v)_{capture}$	Fowler et al 1967
$^3He(n,\gamma)^4He$	$\lesssim 1$ MeV	$(\sigma v)_{capture}$	Fowler et al 1967
$^3He(n,d)D$	$0.1-10$ MeV	σ_{total}	Nuclear Cross Sections
$^3He(\gamma,p)D$	$5.5-$ MeV	$\sigma^{photodiss}$	Gorbunov and Varfolomeev 1964
$^3He(\gamma,n)2p$	$7.7-$ MeV	$\sigma^{photodiss}$	Gorbunov and Varfolomeev 1964
$^3H(\gamma,n)D$	$5.5-$ MeV	$\sigma^{photodiss}$	Faul et al 1981
$^3H(\gamma,p)2n$	$7.7-$ MeV	$\sigma^{photodiss}$	Faul et al 1981
$^4He(\gamma,pn)D$	$25-$ MeV	$\sigma^{photodiss}$	Gorbunov and Spiridonov 1958a
$^4He(\gamma,n)^3He$	$20.6-$ MeV	$\sigma^{photodiss}$	Gorbunov and Spiridonov 1958b
$^4He(\gamma,p)^3H$	$19.8-$ MeV	$\sigma^{photodiss}$	Gorbunov and Spiridonov 1958b
$^4He(\gamma,\ )$	$20-$ MeV	$\sigma^{photodiss}_{total}$	Gorbunov and Spiridonov 1958b
$D(\gamma,n)p$	$2.2-$ MeV	$\sigma^{photodiss}_{total}$	Govarets et al 1981

Reaction	Energy Range	Useful Data	Reference
$^6Li(\gamma,\ )$n	5− MeV	$\sigma^{photodiss}$	Berman 1975
$^6Li(\gamma,\ )$p	5− MeV	$\sigma^{photodiss}$	assumed equal to $^6Li(\gamma,\ )$n
$^6Li(\gamma,\ )^3He,^3H$	18− MeV	$\sigma^{photodiss}$	Wong et al 1970
$^7Li(\gamma,p)^6He$	10− MeV	$\sigma^{photodiss}$	Berman 1975
$^7Li(\gamma,\ )$n,2n	7− MeV	$\sigma^{photodiss}$	Berman 1975
$^7Li(\gamma,t)^4He$	2.5− MeV	$\sigma^{photodiss}$	Berman 1975
$^7Be(\gamma,\ )$	3− MeV	$\sigma^{photodiss}$	assumed same as ^7Li
$n(p,\gamma)d$	$\lesssim$ 1 MeV	$(\sigma v)_{capture}$	Fowler et al 1967
$n(d,\gamma)^3H$	$\lesssim$ 1 MeV	$(\sigma v)_{capture}$	Fowler et al 1967
np, pp	1 MeV-10 GeV	$\sigma_{elastic}, \sigma_{inelastic}, \frac{d\sigma}{d\Omega}^{elastic}$	Meyer 1972
$p-^4He$	1 MeV-10 GeV	$\sigma_{elastic}, \sigma_{inelastic}$	Meyer 1972
$p(^4He,\ )d,^3He,^3H$	1 MeV-10 GeV	$\sigma_{partial}$	Meyer 1972
$p-^4He$	3 MeV-1 GeV	$\frac{d\sigma}{d\Omega}^{elastic}$	Meyer 1972
$p-^4He$	0.6-1.8 GeV	$\frac{d\sigma}{d\Omega}^{elastic}$	Klem et al 1977
$p-d$	1 MeV-10 GeV	$\sigma_{elastic}, \sigma_{inelastic}$	Meyer 1972
$p-^3He$	1 MeV-10 GeV	$\sigma_{elastic}, \sigma_{inelastic}$	Meyer 1972
$n(^4He,pn)^3H$	90,300 MeV	$\frac{d\sigma}{dE_{^3H}}$	Meyer 1972

Table 4. Primordial, astrated and SBBN abundances

	D	^3He	^6Li	^7Li
Primordial	6.4×10^{-5}	1.2×10^{-4}	2.6×10^{-10}	8.4×10^{-11}
Primordial SBBN	few 10^{-5}	$\leq$ few 10^{-5}	$< 10^{-11}$	10^{-10}
Disk: 50%	3.2×10^{-5}	7.5×10^{-5}	1.3×10^{-10}	(10^{-9})
Disk: 75%	1.6×10^{-5}	5.2×10^{-5}	6.5×10^{-11}	(10^{-9})
Disk: 90%	0.6×10^{-5}	3.9×10^{-5}	2.6×10^{-11}	(10^{-9})
SBBN	few 10^{-5}	$\leq$ few 10^{-5}	$< 10^{-11}$	(10^{-9})
Observation	$8 \times 10^{-5} - 4 \times 10^{-4}$	$10^{-5} - 4 \times 10^{-4}$	$< 10^{-10}$	10^{-9}

Primordial and astrated abundances of D, ^3He, ^6Li and ^7Li in a decaying particle scenario with $M_x/r_B^* = 7 \times 10^4$GeV, $\tau_X = 4.5 \times 10^5$s and $\xi_7 = 1.7\xi_7^c$, compared with observations and with the predictions of Standard Big Bang Nucleosynthesis.

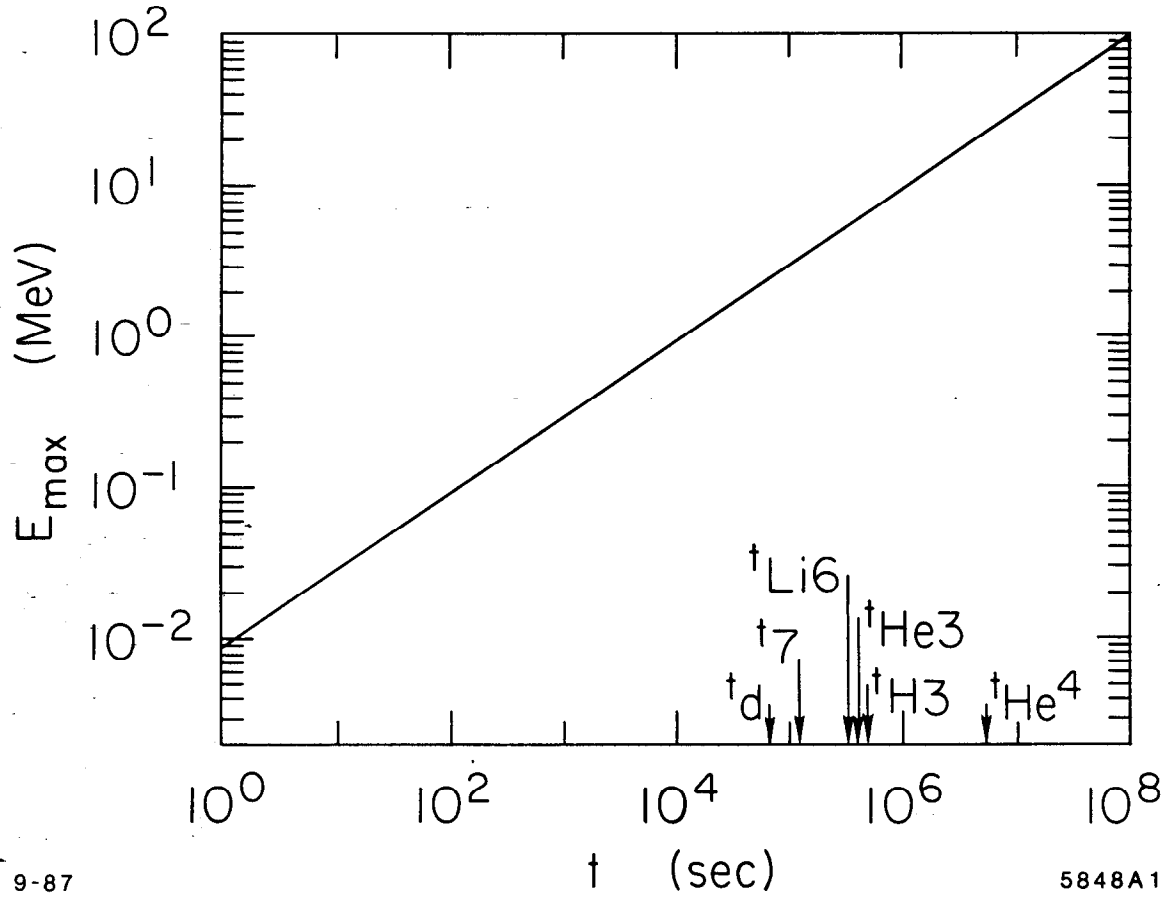
10^2
10^1
10^0
10^{-1}
10^{-2}
E_{max} (MeV)
$^tLi6$
$^t7$
$^tHe3$
^td
$^tH3$
$^tHe^4$
10^0
10^2
10^4
10^6
10^8
t (sec)
9-87
5848A1

Fig. 1

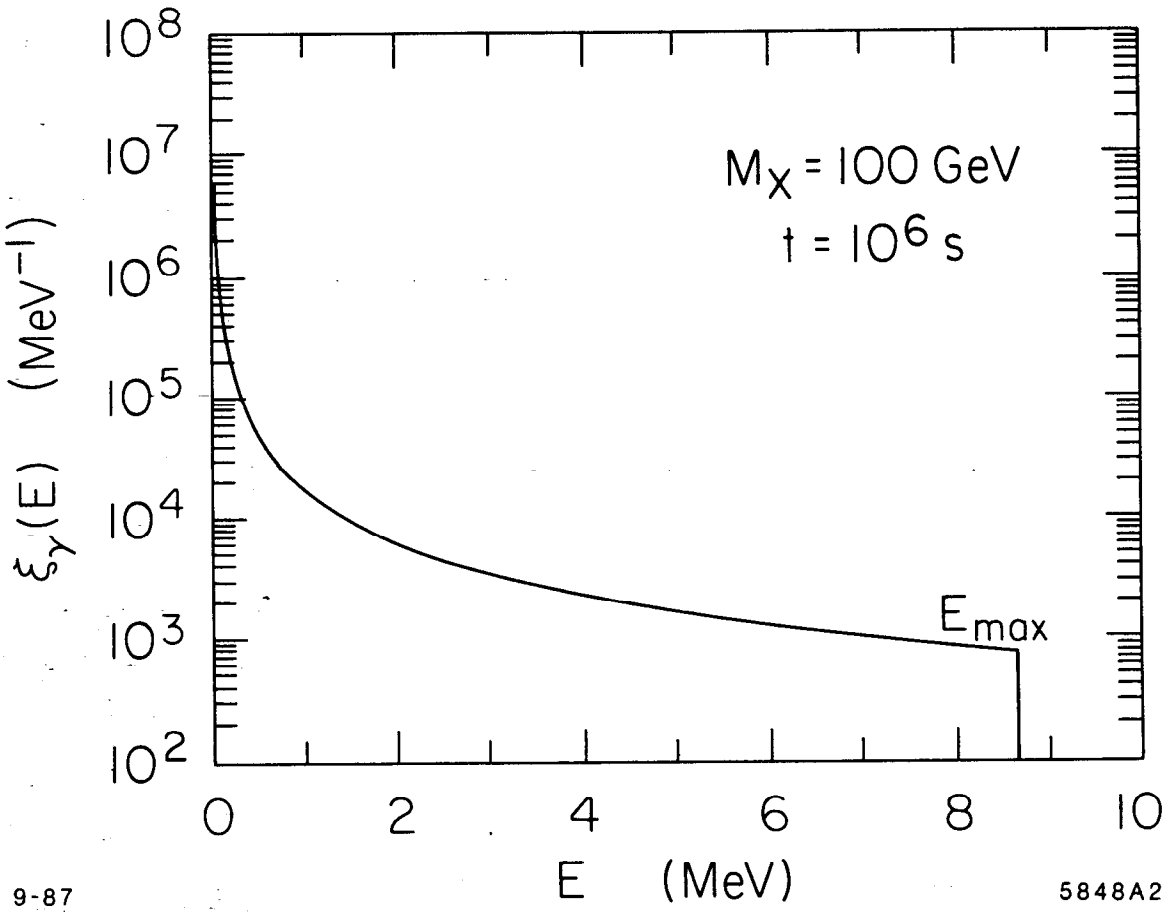
10^8
10^7
10^6
10^5
10^4
10^3
10^2
$\xi_\gamma(E)$ (MeV^{-1})
M_X = 100 GeV
$t = 10^6$ s
E_{max}
0
2
4
6
8
10
E (MeV)
9-87
5848A2

Fig. 2

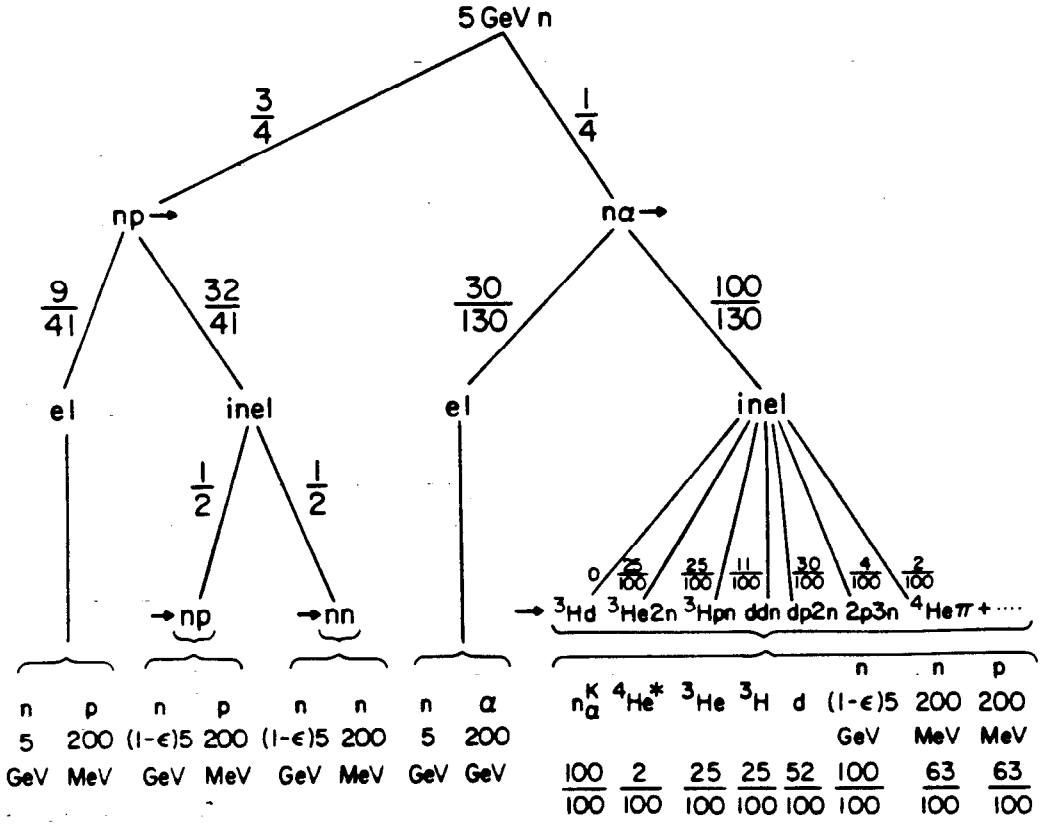

TOTALS:

$$n(E = 5\,\text{GeV}) : \frac{9}{41}\frac{3}{4} + \frac{30}{130}\frac{1}{4} = 0.22$$

$$n[E = (1-\epsilon)5\,\text{GeV}] : \frac{32}{41}\frac{3}{4} + \frac{100}{130}\frac{1}{4} = 0.65$$

$$n(E = 200\,\text{MeV}) : \frac{16}{41}\frac{3}{4} + \frac{63}{130}\frac{1}{4} = 0.41$$

$$p(E = 200\,\text{MeV}) : \frac{25}{41}\frac{3}{4} + \frac{63}{130}\frac{1}{4} = 0.58$$

$$n_\alpha^K : \frac{100}{130}\frac{1}{4} = 0.19$$

$$^4\text{He} : \frac{32}{130}\frac{1}{4} = 0.06$$

$$^3\text{He} : \frac{25}{130}\frac{1}{4} = 0.05$$

$$^3\text{H} : \frac{25}{130}\frac{1}{4} = 0.05$$

$$d : \frac{52}{130}\frac{1}{4} = 0.10$$

8-87

5848A3

Fig. 3

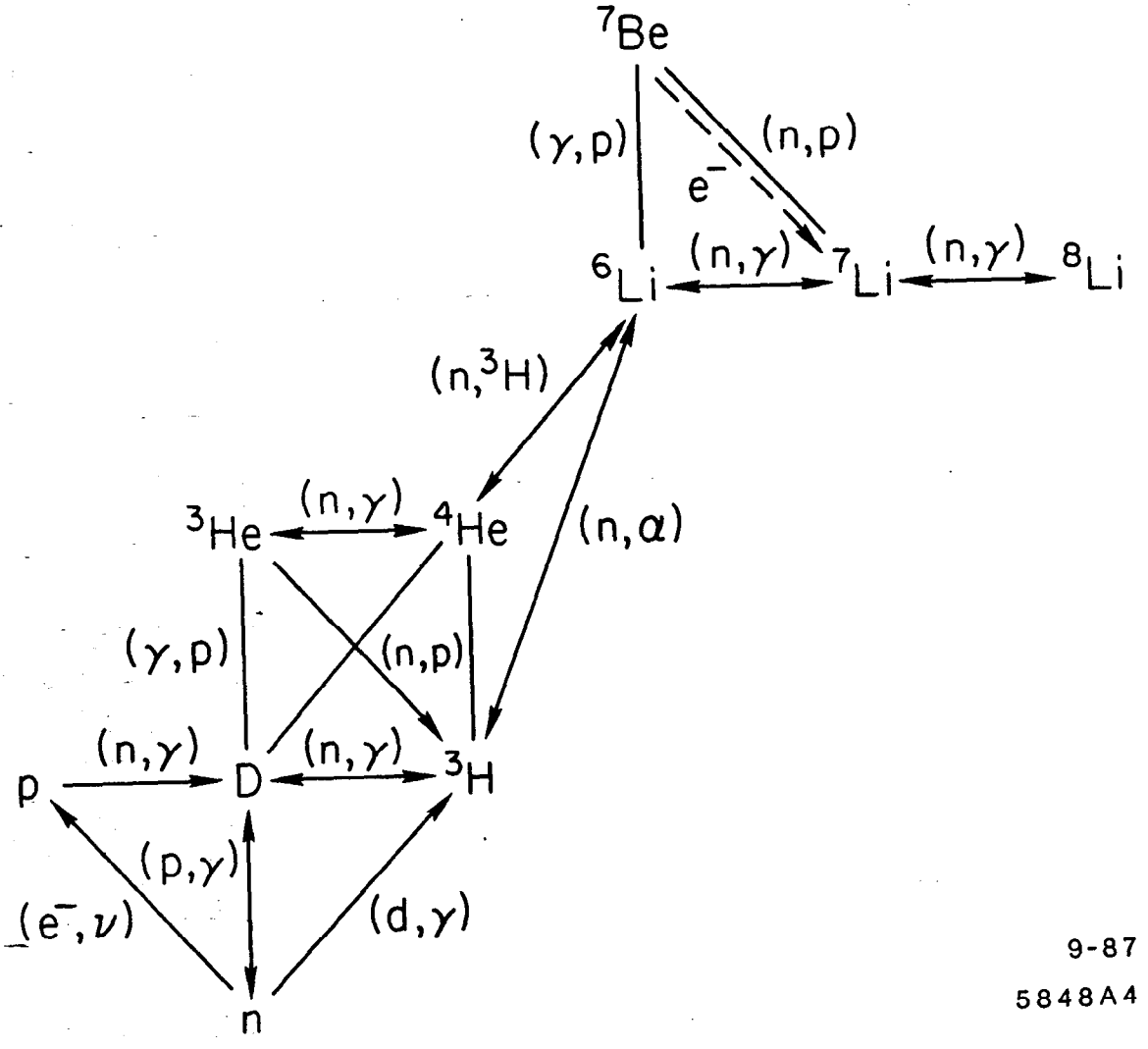
^{7}Be
(γ,p)
(n,p)
e⁻
^{6}Li
(n,γ)
^{7}Li
(n,γ)
^{8}Li
(n,^{3}H)
^{3}He
(n,γ)
^{4}He
(n,α)
(γ,p)
(n,p)
p
(n,γ)
D
(n,γ)
^{3}H
(p,γ)
(e⁻,ν)
(d,γ)
n
9-87
5848A4

Fig. 4

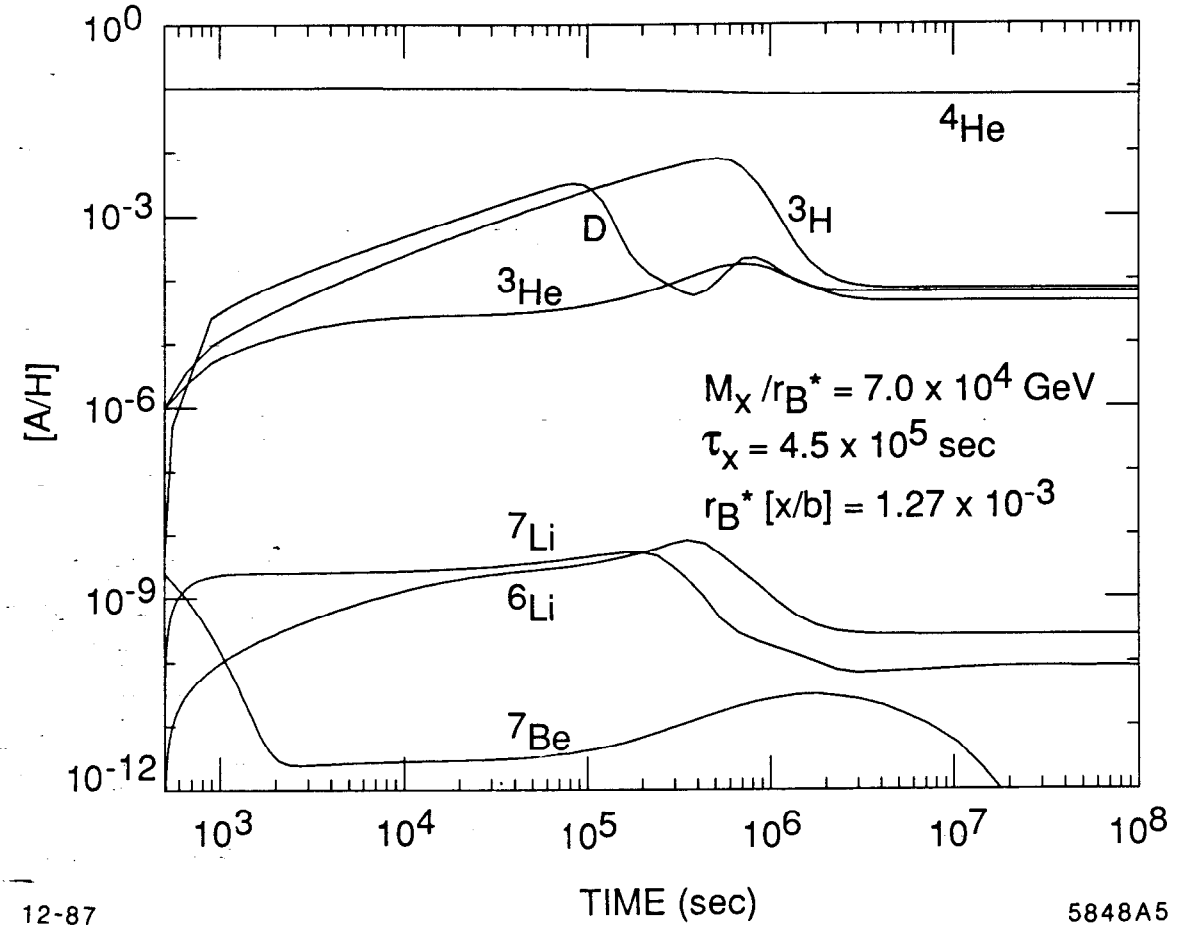
10^0
10^{-3}
10^{-6}
10^{-9}
10^{-12}
[A/H]
^{4}He
^{3}H
D
^{3}He
$M_X / r_B^* = 7.0 \times 10^4$ GeV
$\tau_X = 4.5 \times 10^5$ sec
r_B^* [x/b] = 1.27×10^{-3}
^{7}Li
^{6}Li
^{7}Be
10^3
10^4
10^5
10^6
10^7
10^8
TIME (sec)
12-87
5848A5

Fig. 5

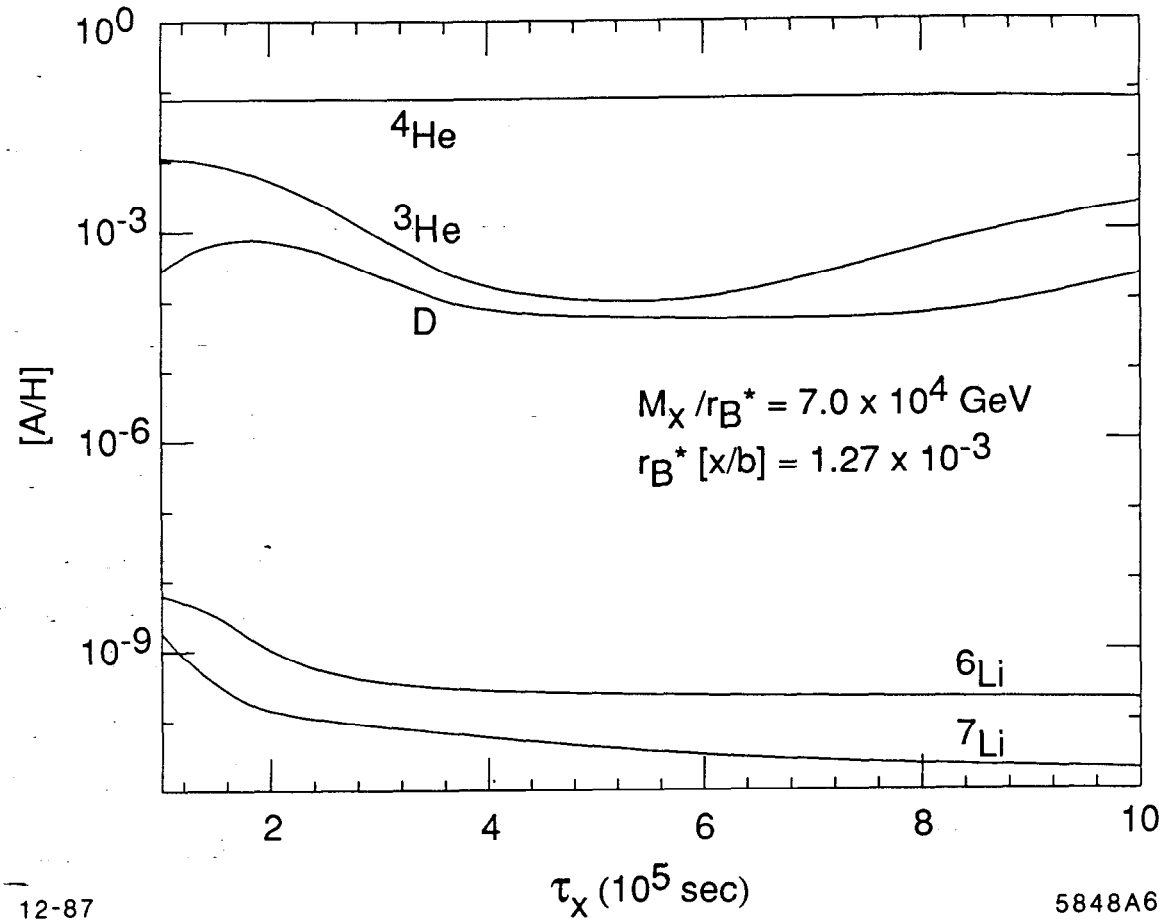
10^0
10^{-3}
10^{-6}
10^{-9}
[A/H]
^{4}He
^{3}He
D
$M_X / r_B^* = 7.0 \times 10^4$ GeV
$r_B^* [x/b] = 1.27 \times 10^{-3}$
^{6}Li
^{7}Li
2
4
6
8
10
τ_X (10^5 sec)
12-87
5848A6

Fig. 6

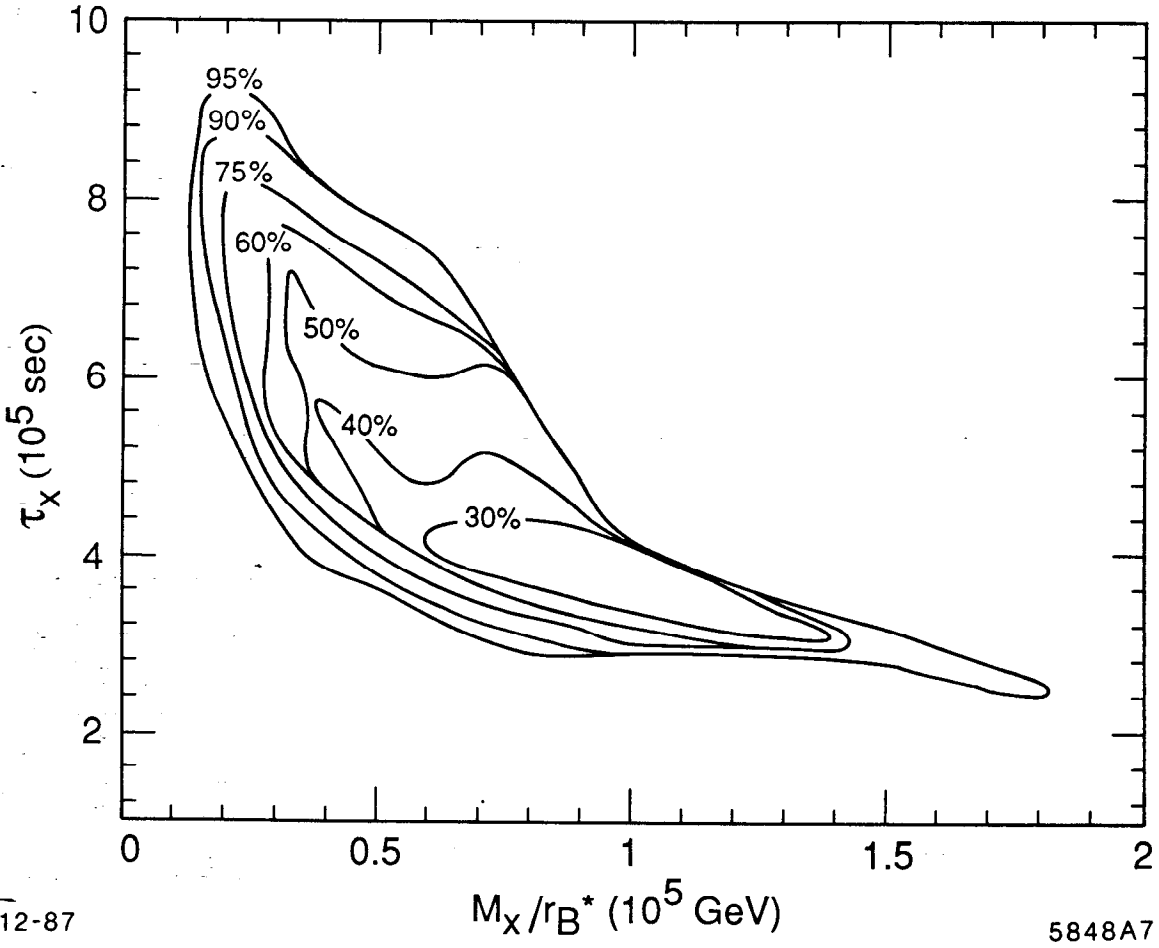
95%
90%
75%
60%
50%
40%
30%
10
8
6
4
2
0
0.5
1
1.5
2
τ_X (10^5 sec)
M_X/r_{B^*} (10^5 GeV)
12-87
5848A7

Fig. 7

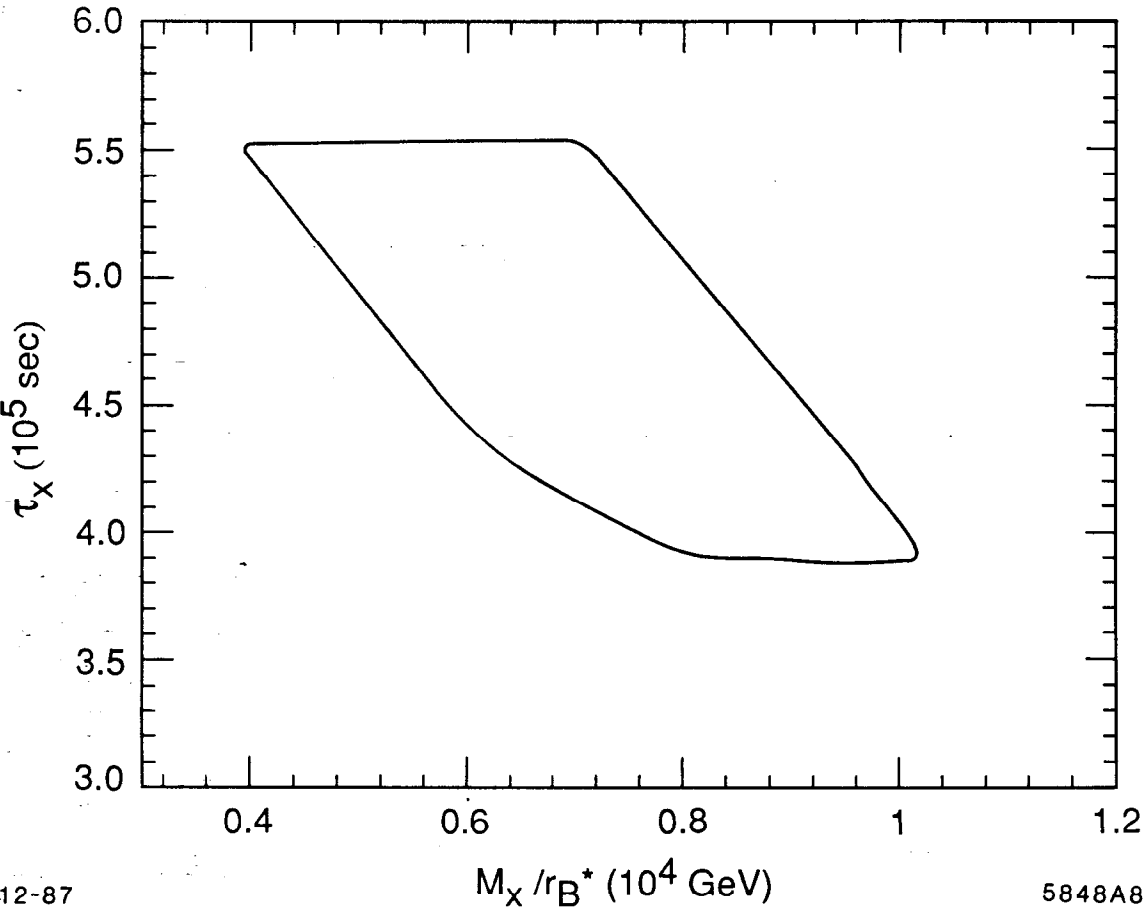
6.0
5.5
5.0
4.5
4.0
3.5
3.0
τ_X (10^5 sec)
0.4
0.6
0.8
1
1.2
M_X / r_{B^*} (10^4 GeV)
12-87
5848A8

Fig. 8

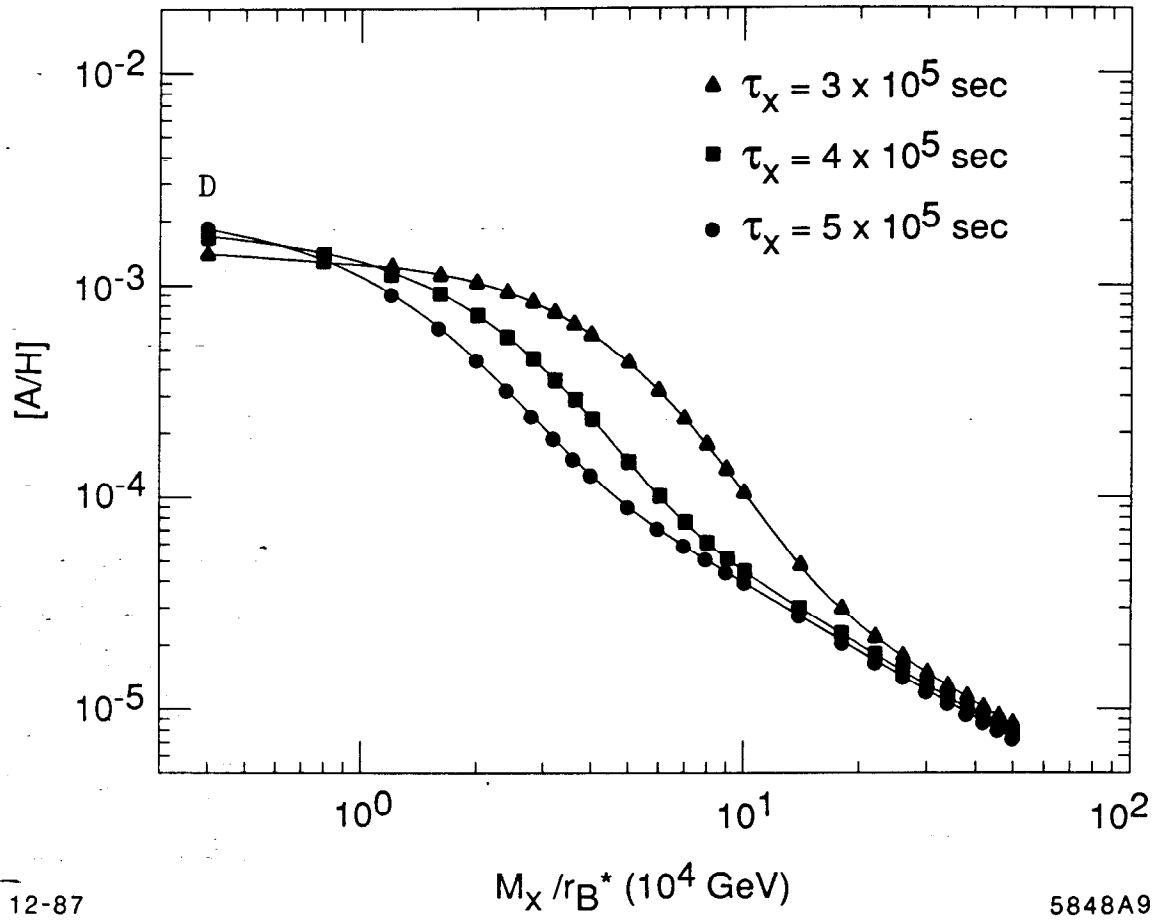
10^{-2}
10^{-3}
10^{-4}
10^{-5}
[A/H]
D
$\tau_x = 3 \times 10^5$ sec
$\tau_x = 4 \times 10^5$ sec
$\tau_x = 5 \times 10^5$ sec
10^0
10^1
10^2
M_X / r_B^* (10^4 GeV)
12-87
5848A9

Fig. 9a

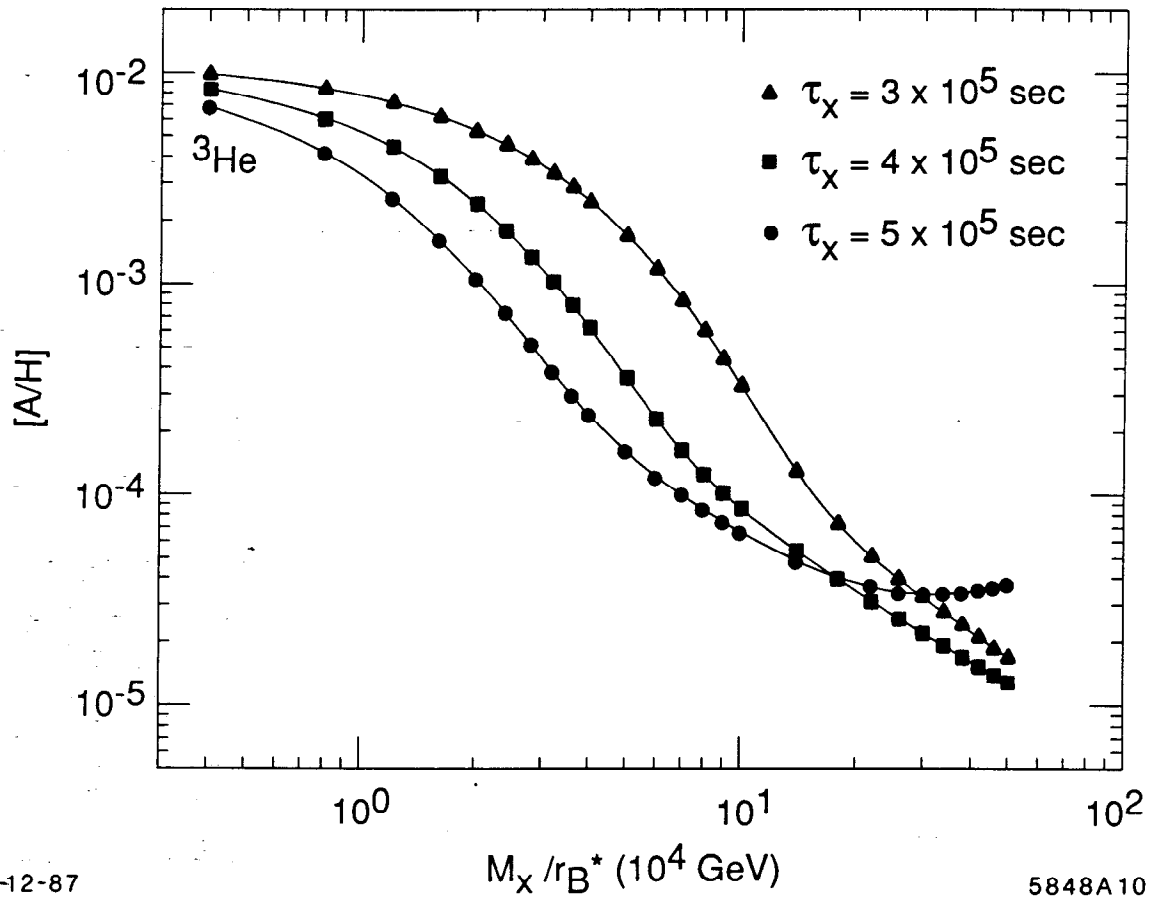
10^{-2}
10^{-3}
10^{-4}
10^{-5}
[A/H]
^{3}He
$\tau_x = 3 \times 10^5$ sec
$\tau_x = 4 \times 10^5$ sec
$\tau_x = 5 \times 10^5$ sec
10^0
10^1
10^2
M_x / r_B^* (10^4 GeV)
12-87
5848A10

Fig. 9b

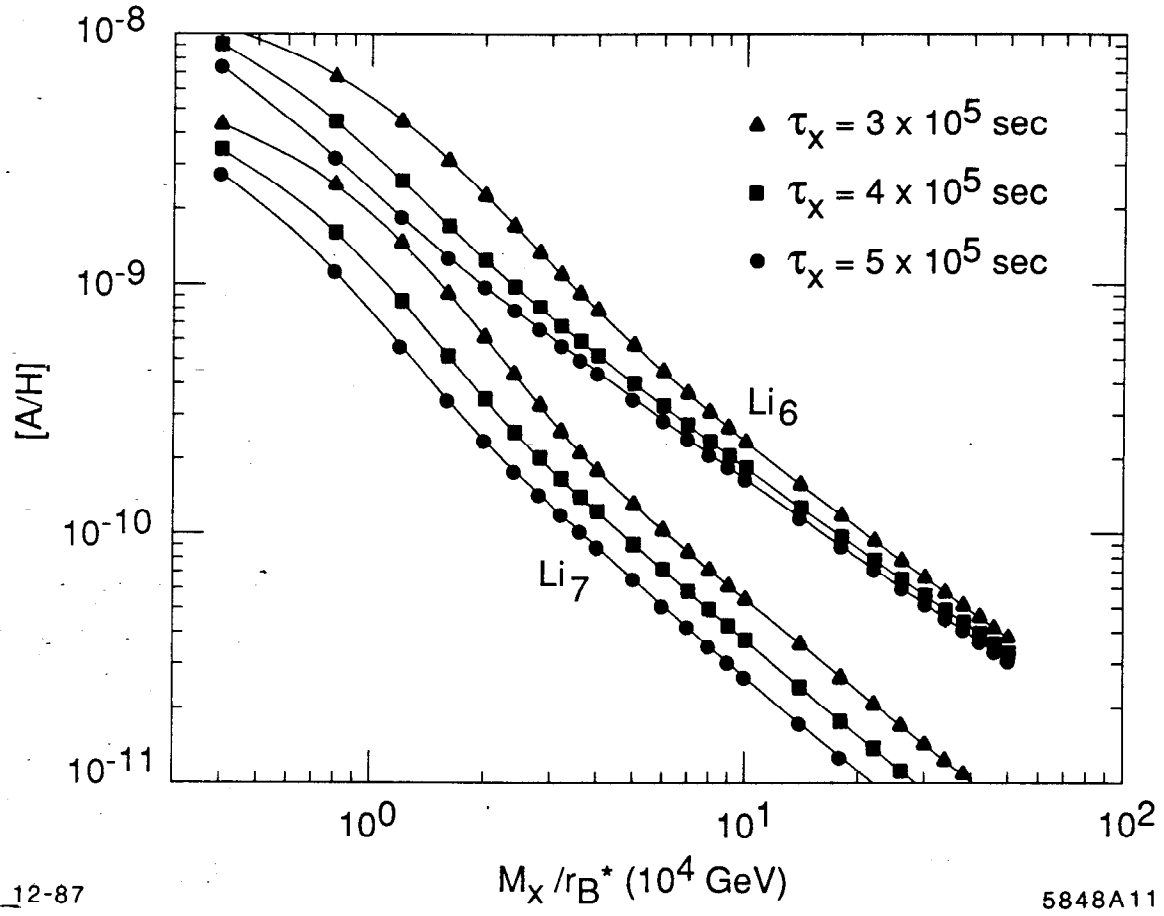
10^{-8}
10^{-9}
10^{-10}
10^{-11}
[A/H]
$\tau_x = 3 \times 10^5$ sec
$\tau_x = 4 \times 10^5$ sec
$\tau_x = 5 \times 10^5$ sec
Li_6
Li_7
10^0
10^1
10^2
M_x / r_B^* (10^4 GeV)
12-87
5848A11

Fig. 9c